МОСКОВСКИЙ ГОСУДАРСТВЕННЫЙ
ИНЖЕНЕРНО-ФИЗИЧЕСКИЙ ИНСТИТУТ
(ТЕХНИЧЕСКИЙ УНИВЕРСИТЕТ)

**S.G. Rubin** **A.G. Terekidi**

**024-97**



# BIPOLARON THEORY AND ITS APPLICATION IN $YBA_2CU_3O_{6+x}$

**Moscow 1997**

RUSSIAN FEDERATION STATE COMMITTEE
OF HIGHER EDUCATION

MOSCOW STATE ENGINEERING PHYSICS INSTITUTE
(TECHNICAL UNIVERSITY)

S.G. RUBIN A.G. TEREKIDI

# BIPOLARON THEORY AND ITS APPLICATION IN $YBA_2CU_3O_{6+x}$

Preprint 024-97



Moscow 1997

UDC 538.945

R88

Всего: 1 экз.

S.G. Rubin, A.G. Terekidi. Bipolaron theory and its application in $YBA_2CU_3O_{6+x}$.
Moscow: Preprint / MSEPI, 024-97, 1997.--60p.

ABSTRACT

A system of strongly interacting fermions in a solid state is discussed. A structure of singlet and triplet coupled 2-particle states and their excitation spectra are investigated. It is shown that an account of intersite fermion interaction leads to new boson modes. Their number depends on dimensionality of a system. It is shown also that a reasonable choice of Hamiltonian parameters leads to a small effective mass of local pairs. A problem of interaction of coupled states with external fields is discussed. The calculations are carried out for intermediate and strong fermion - fermion coupling. Several independent experiments are explained on the basis of developed formalism.



ISBN 5-7262-0159-0

# Contents

# 1. Introduction

The discovery of high-temperature superconductors (HTSC) that differ drastically from conventional superconductors leads to a great number of theoretical models. A small coherence length in HTSC–materials indicates that a size of fermion pairs, which is crucial for the superconducting properties, should be of the order of lattice parameter.

In this paper the formalism of tightly binding fermions in solids is developed. The main tool is extended Hubbard model with a fermion-fermion intersite attraction. The origin of the attraction could be 'phononic', 'excitonic' [1], 'plasmonic' [2] or 'magnonic' [3].

Last years indicate the power of the bipolaron theory [4], [5] and we shall identify the local pairs and bipolarons – local pairs with phonon mechanism of 2-fermion attraction. The presence of the attraction changes the band structure significantly. Fermions being placed on different sites are coupled into pairs. The continuum of electron-hole pairs is situated above the local pair bands and does not overlap with them both in the normal and superconducting phases – see discussion in [6]. It is the main difference of BCS-like theories and local pair ones.

The pair size seems to be of the same order of the distance between pairs that appears to be rather difficult for theoretical analysis. Nevertheless there are some papers [6], [7] that are devoted to this complex intermediate region of crossover from Cooper pair regime to local pair one.

A presence of a superconducting state indicates an existence of boson type excitations, that are able to form a condensate at low temperatures. But there are fermions (electrons) in solids as the only charge carriers from the beginning that interact with phonons and other quasiparticles in crystal. This interaction in HTSC – materials is very complicated both for experimental and theoretical investigations. As a result, a large variety of superconductivity models has been developed. Most of papers deal with a ground state and excitation spectra on the basis of an attractive or repulsive Hubbard model (see review [8]). Although a generalization to a more realistic and complicated situation is not obvious, several interesting papers have been recently appeared [6], [9], [10]. In [9] the authors detaily considered a ground state of such a system with rather general form of interaction in site representation. In [10] the Green function

method was applied to the boson spectra excitations. But the latter work was motivated by Auger experiments in noble metals and only fermion – fermion repulsion was taken into account.

It seems evident that future theory of the superconductivity should include several issues:

a. Determination of an effective charge carrier with fermi-statistics and a form of a Hamiltonian.

b. Investigation of the boson excitations - band structure, interaction with each other and with external fields.

c. Experimental determination of Hamiltonian parameters.

This work is completely devoted to the issue b). We start with rather general form of fermion – fermion interaction to be able to describe a large variety of interaction forms in different HTSC – materials. To be more definite, we postulate the effective Hamiltonian for fermi excitations in site representation in the form:

$$H = -\mu \sum_M c_M^+ c_M + \sum_{M,N} t(\mathbf{m}-\mathbf{n}) c_M^+ c_N +$$

$$+\frac{1}{4} \sum_{MNM'N'} U_{MN,M'N'} c_M^+ c_N^+ c_{M'} c_{N'} + \sum_{MN} B_{MN} c_M^+ c_N . \qquad (1)$$

Here $\mu$ is the chemical potential, and for example $M = (\mathbf{m}, s)$, where $\mathbf{m}$ represents the site index, $s$ is the spin projection of the fermion, $c_M^+, c_M$ are the operators for fermion creation and annihilation on the site $\mathbf{m}$ with the spin projection $s = \pm\frac{1}{2}$, $U_{MN,M'N'}$ - is the matrix element of fermion interaction. This matrix is antisymmetric in its first and second pairs of indices separately: $U_{MN,M'N'} = -U_{NM,M'N'} = -U_{MN,N'M'}$. A hopping integral $t(\mathbf{m}-\mathbf{n})$ characterizes the fermion motion and describes a kinetic energy in a momentum representation. $B_{MN}$ represents an arbitrary external field.

It must be stressed here that only fermi statistics of primordial quasiparticles is important. One can keep in mind polarons, holes, magnons and so on. The question is if the interaction is strong enough to form the local pairs or we have Cooper pairs in high-$T_c$ superconductors as in the ordinary ones. A mathematical method in the latter case has been developed quite accurately. The method, developed in this paper for the description

of the local pairs is based on a functional integral technique [11], that was widely used in different theoretical investigations (see, for example, [12], [17], [13]). It was applied to a single-polaron problem [14] and is used here for the local pair description of strongly interacting fermions. Calculations appear to be rather simple in the case of short - distance interaction. Furthermore mathematical difficulties increase slightly with a number of accounted sites.

Below the general formalism is presented for an arbitrary form of fermion – fermion interaction. Detailed calculations of spectra excitations and a structure of the pairs are discussed.

# 2. General formalism

## 2.1. Main equations

The Hamiltonian $H$ in the form (1) is quite general and its origin is not discussed here. The external field $B$ is written in a general form too. This form includes the interaction with electromagnetic field and neutrons, for example. Let's start with partition function of the system in a functional integral form [12]:

$$Z = Spe^{-\beta H} = \int Dc^* Dc \exp S[c^*, c],$$

$$S[c^*, c] = \int_0^\beta d\tau [\sum_A c^*{}_A \dot{c}_A - H(c^*, c)] = \int_0^\beta d\tau [\sum_A c_A^* \dot{c}_A +$$

$$+ \sum_{AB} \tau_{AB} c_A^* c_B - \sum_{ABA'B'} \frac{1}{4} U_{AB;A'B'} c_A^* c_B^* c_{A'} c_{B'}], \qquad (2)$$

$$\tau_{AB} = (\mu - \omega_{p_A})\delta_{AB}.$$

Expression (2) is written in momentum representation where complex index $A = (p_A, s_A)$ includes quasimomentum and spin projection of a fermion; $\omega_{p_A}$ is the fermion spectrum determined as a Fourier transform of the hopping integral; $c_A^*(\tau), c_A(\tau)$ are independent grassman variables; $\beta = 1/T$ is the inverse temperature. The external field $B$ is omitted in this section. To get rid of the four grassman variables product in the exponent

and introduce the bosonic variables $\psi_{AB}(\tau)$ one can use the Hubbard – Stratonovich transformation [15], [7] which is usually applied to consideration of bosonic fields of one argument that describes boson motion as a whole. In this latter case all the information about the internal structure of the bound state is lost, though the results of conventional BCS – theory of superconductivity are reproduced [12], [16]. But as far as we intend to study the internal pair structure and the interaction of the pairs with external fields we should use more complex bosonic fields $\psi_{AB}(\tau), \psi_{AB}(\tau)^*$. In this case expression (2) is transformed into:

$$Z = \int Dc^* DcD\psi^* D\psi e^{S_e},$$

$$S_e = \int_0^\beta d\tau [\sum_A c_A^* \dot{c}_A + \sum_{AB} \left[ r_{AB} c_A^* c_B + \frac{1}{2}\psi_{AB}^* c_A c_B + \frac{1}{2}\psi_{AB} c_A^* c_B^* \right] +$$

$$+ \sum_{ABA'B'} \psi_{AB}^* U_{AB;A'B'}^{-1} \psi_{A'B'}]. \qquad (3)$$

Our central problem is to obtain equations for the wave functions of the coupled states and to find their solutions for the chosen form of interaction term. An imaginary "time" Fourier – transformation gives:

$$S_e = \sum_{\epsilon AB} (r_{AB} + i\epsilon\delta_{AB}) c_A^*(\epsilon) c_B(\epsilon) + \frac{1}{2} \sum_{\epsilon\epsilon' AB} \psi_{AB}^*(\epsilon + \epsilon') c_A(\epsilon) c_B(\epsilon') +$$

$$+ \frac{1}{2} \sum_{\epsilon\epsilon' AB} \psi_{AB}(\epsilon + \epsilon') c_A^*(\epsilon) c_B^*(\epsilon') + \sum_{EABA'B'} \psi_{AB}^*(E) U_{AB;A'B'}^{-1} \psi_{A'B'}(E),$$

where Matsubara frequencies $\epsilon = (2n+1)\pi/\beta, \epsilon' = (2n'+1)\pi/\beta$ due to antiperiodic boundary conditions for fermionic variables and $E = 2\pi n/\beta$ due to periodic boundary conditions for boson dynamic variables. Now one can integrate out the grassman variables [12]:

$$Z = \int D\psi^* D\psi e^{S_b},$$

$$S_b = \sum_{ABA'B'E} \psi_{AB}^*(E) U_{AB;A'B'}^{-1} \psi_{A'B'}(E) + Tr(lnY), \qquad (4)$$

$$Y_{AB}(\epsilon, \epsilon') = \begin{pmatrix} (r_{AB} + i\epsilon\delta_{AB})\delta_{\epsilon,\epsilon'} & \psi_{AB}(\epsilon + \epsilon') \\ \psi_{AB}^*(\epsilon + \epsilon') & -(r_{AB} + i\epsilon\delta_{AB})\delta_{\epsilon,\epsilon'} \end{pmatrix}.$$

Boson dynamic variables $\psi^*_{AB}, \psi_{AB}$ having been introduced, the expression (4) remains not very suitable for the further analysis. Next step is to expand the action $S_b$ around a classical action $S_b[\psi_{cl}]$. ($\delta S_b/\delta\psi_{cl} = 0$ by definition). The simplest case $\psi_{cl} = 0$, takes place: a) in a normal phase (by definition), b) near critical temperature, where a condensate density is small, and c) in a low fermion density limit. Calculations for $\psi_{cl} \neq 0$ were discussed in [17]. Here we will be interested in the normal phase of the system.

Let's expand the effective action $S_b$ (4) in Tailor series up to the second order in fields $\psi^*_{AB}, \psi_{AB}$ around trivial classical trajectory $\psi_{cl} = 0$. A fourth order in the fluctuation describes interaction of pairs and was discussed in [18]. As it was shown in ref. [19], this term is small in a low density region and/or for a weak fermion interaction. Here we neglect the pair interaction and limit ourselves to the study of boson excitation spectra and their interaction with external fields. Simple, but tedious calculations lead to quadratic part of the effective boson action:

$$S_b^{(2)} = \sum_{ABA'B'E} \psi^*_{AB}(E)\tilde{D}_{AB,A'B'}(E)\psi_{A'B'}(E),$$

$$\tilde{D}_{AB,A'B'}(E) = \tfrac{1}{4}\frac{th(\beta\Omega_A/2)+th(\beta\Omega_B/2)}{-iE+\Omega_A+\Omega_B}\delta_{AB'}\delta_{A'B} + U^{-1}_{A'B';AB},$$

$$\Omega_A = \omega_{\mathbf{p}A} - \mu.$$

To remove the denominator in the first term and the inverse power of the interaction operator U, one has to make the following substitution of variables in the functional integral (4): $U^{-1}\psi \to \psi, \psi^*_{AB} \cdot (iE\Omega_A - \Omega_B) \to \psi^*_{AB}$, . This procedure leads to the partition function in the form:

$$Z = \int D\psi^* D\psi \exp\{\sum_{ABA'B'E} \psi^*_{AB}(-D_{AB,A'B'} + iE\delta_{AA'}\delta_{BB'})\psi_{A'B'}\}, \quad (5)$$

where

$$D_{AB,A'B'} = (\Omega_A + \Omega_B)\delta_{AA'}\delta_{BB'} + W_{AB,B'A'}, \quad (6)$$

$$W_{AB;B'A'} = \frac{1}{4}\cdot(th\frac{\beta\Omega_A}{2} + th\frac{\beta\Omega_B}{2})U_{AB;B'A'}. \quad (7)$$

Now we have to diagonalize the quadratic form of the exponent, that is to

solve the equation:

$$\sum_{A'B'} D_{AB;A'B'} u^{(n)}_{A'B'} = \lambda_n u^{(n)}_{AB}. \tag{8}$$

Complex index $n$ numerating the eigenstates of the system will be shown to include quasimomentum of the local pair, its spin and a band number. The eigenvalues $\lambda_n$ obey the secular equation:

$$Det(D_{AB;A'B'} - \lambda_n \delta_{AA'}\delta_{BB'}) = 0. \tag{9}$$

The eigenfunctions are chosen to be orthonormal:

$$\sum_{AB} u^{(n)*}_{AB} u^{(n')}_{AB} = \delta_{nn'}. \tag{10}$$

The final step consists of introducing new variables $C_n(E)$ in the integral (5):

$$\psi_{AB} = \sum_n C_n(E) u^{(n)}_{AB};\ \psi^*_{AB} = \sum_n C^*_n(E) u^{(n)*}_{AB}.$$

This leads to the expression:

$$Z = \prod_n \int DC^*_n DC_n \exp\{C^*_n(iE - \lambda_n)C_n\}. \tag{11}$$

This form of the partition function clarifies the meaning of the new variables $C^*_n, C_n$ as the wave functions of bosonic excitations of energy $\lambda_n$. It will be shown below that $u^{(n)}_{AB}$ functions describing the internal structure of the bound state must be taken into account in the analysis of the pair interaction with an external field. Eq.(9) is the only one we need to calculate bosonic - type spectra excitations. The pair energy depends on its quasimomentum and spin projection. Quasimomentum and spin conservation can be accounted for in the form of interaction term:

$$W_{AB,B'A'} = \frac{1}{4} w_{AB,B'A'} \delta(A + B - A' - B'). \tag{12}$$

Index $A = (\mathbf{p}_A, s_A)$ includes both the momentum $\mathbf{p}_A$ and the spin projection $s_A$ of the fermion. Let variables $R = A + B$, $R' = A' + B'$ characterize the momentum and spin projection of the coupled state as a whole. One

can easily find from Eqs.(6,12), that matrix $D$ is diagonal in indices $R, R'$. Several energy bands may exist and we specify them by additional index $\alpha$. It means that the complex index $n$ in the expression (11) should incorporate the quasimomentum $\mathbf{p}_K$ of the 2-particle state as well as its spin projection $\sigma_K = 0, \pm 1$, united in the common index $K = (\mathbf{p}_K, \sigma_K)$, and eigenfunctions of the matrix $D$ should have the form:

$$u_{AB}^{(n)} \equiv v_{RA}^{(n)} = v_{RA}^{(\kappa,\alpha,K)} = \delta_{K,R} x_{KA}^{(\kappa,\alpha)}, \tag{13}$$

where $\kappa = 0(1)$ corresponds to singlet (triplet) case. The substitution of expression (13) into Eq.(8) along with the normalization condition term (10) lead to:

$$[\Omega_A + \Omega_{K-A} - \lambda_\alpha(K)] x_{KA}^{(\kappa,\alpha)} + \frac{1}{4} \sum_{A'} w_{A,K-A;K-A',A'} x_{KA'}^{(\kappa,\alpha)} = 0, \tag{14}$$

and

$$\sum_A x_{KA}^{(\kappa,\alpha)*} x_{KA}^{(\kappa',\alpha')} = \delta_{\kappa\kappa'} \delta_{\alpha\alpha'}. \tag{15}$$

These equations determine the pair structure $x_{KA}^{(\kappa,\alpha)}$ and the excitation spectra $\lambda_{\kappa,\alpha}(K)$. The previous analysis shows that for $\kappa = 0$ the solution is antisymmetrical in the fermion spin indices ($x_{K,A}^{(0,\alpha)} = -x_{K,K-A}^{(0,\alpha)}$) while it is symmetrical for $\kappa = 1$. It confirms the notation $\kappa = 0$ for the singlet pairs and $\kappa = 1$ for the triplet ones.

## 2.2. Equations for triplet and singlet states

Cooper pairs in the BCS theory are singlets. There are many reasons to think that in HTSC - materials triplet pairs exist along with singlet ones [20]. Both of these possibilities are included in the system of equations (14) and the task is to write down the equations for the singlet and triplet states separately. It is convenient to redefine the wave functions of the coupled states and the interaction term $w$ by extracting the spin variables, that are included in the indices $A$, $A'$ and so on:

$$x_{\sigma,s}^{(\kappa,\alpha)}(\mathbf{k},\mathbf{p}) \equiv x_{KA}^{(\kappa,\alpha)},$$

$$w_{s,\sigma-s,\sigma-s',s'}(\mathbf{p},\mathbf{k}-\mathbf{p};\mathbf{k}-\mathbf{p}',\mathbf{p}') \equiv w_{A,K-A;K-A',A'}$$

Here as usual: $K = (\mathbf{k}, \sigma); A = (\mathbf{p}, s); A = (\mathbf{p}', s'); \sigma = 0, \pm 1; s = \pm\frac{1}{2}$. Lower (spin) indices of the interaction $w$ are restricted to the values $\pm\frac{1}{2}$ by definition.

Let us rewrite Eq.(14) using these notations for each spin projection $\sigma$ of a coupled state. The equation for $\sigma = 1$ becomes:

$$[\Omega_{\mathbf{p}} + \Omega_{\mathbf{k}-\mathbf{p}} - \lambda_\alpha(K)] x^{(1,\alpha)}_{1,\frac{1}{2}}(\mathbf{k}, \mathbf{p}) +$$
$$+ \frac{1}{4} \sum_{\mathbf{p}'} w_{\frac{1}{2},\frac{1}{2};\frac{1}{2},\frac{1}{2}}(\mathbf{p}, \mathbf{k}-\mathbf{p}; \mathbf{k}-\mathbf{p}', \mathbf{p}')\, x^{(1,\alpha)}_{1,\frac{1}{2}}(\mathbf{k}, \mathbf{p}') = 0. \qquad (16)$$

This equation is apparently symmetrical in the spin indices and its solution should describe triplet states. We marked it by setting $\kappa = 1$.

The case $\sigma = 0$ is more complex, because of the contributions from triplet and singlet states. Accordingly, one obtains the system of two equations:

$$[\Omega_{\mathbf{p}} + \Omega_{\mathbf{k}-\mathbf{p}} - \lambda_\alpha(K)] x^{(\kappa,\alpha)}_{0,\frac{1}{2}}(\mathbf{k}, \mathbf{p}) +$$
$$+ \frac{1}{4} \sum_{\mathbf{p}'} [w_{\frac{1}{2},-\frac{1}{2};-\frac{1}{2},\frac{1}{2}}(\mathbf{p}, \mathbf{k}-\mathbf{p}; \mathbf{k}-\mathbf{p}', \mathbf{p}')\, x^{(\kappa,\alpha)}_{0,\frac{1}{2}}(\mathbf{k}, \mathbf{p}') +$$
$$+ w_{\frac{1}{2},-\frac{1}{2};\frac{1}{2},-\frac{1}{2}}(\mathbf{p}, \mathbf{k}-\mathbf{p}; \mathbf{k}-\mathbf{p}', \mathbf{p}')\, x^{(\kappa,\alpha)}_{0,-\frac{1}{2}}(\mathbf{k}, \mathbf{p}')] = 0,$$

$$[\Omega_{\mathbf{p}} + \Omega_{\mathbf{k}-\mathbf{p}} - \lambda_\alpha(K)] x^{(\kappa,\alpha)}_{0,-\frac{1}{2}}(\mathbf{k}, \mathbf{p}) +$$
$$+ \frac{1}{4} \sum_{\mathbf{p}'} [w_{-\frac{1}{2},\frac{1}{2};-\frac{1}{2},\frac{1}{2}}(\mathbf{p}, \mathbf{k}-\mathbf{p}; \mathbf{k}-\mathbf{p}', \mathbf{p}')\, x^{(\kappa,\alpha)}_{0,\frac{1}{2}}(\mathbf{k}, \mathbf{p}') +$$
$$+ w_{-\frac{1}{2},\frac{1}{2};\frac{1}{2},-\frac{1}{2}}(\mathbf{p}, \mathbf{k}-\mathbf{p}; \mathbf{k}-\mathbf{p}', \mathbf{p}')\, x^{(\kappa,\alpha)}_{0,-\frac{1}{2}}(\mathbf{k}, \mathbf{p}')] = 0. \qquad (17)$$

A nontrivial solution to this system exists only if both equations are equivalent. This equivalence is guaranteed by antisymmetrical properties of the $x$ and $w$ functions:

$$x^{(\kappa,\alpha)}_{0,\frac{1}{2}}(\mathbf{k}, \mathbf{p}) = -x^{(\kappa,\alpha)}_{0,-\frac{1}{2}}(\mathbf{k}, \mathbf{k}-\mathbf{p});$$

$$w_{s,s';s'',s'''}(\mathbf{p}, \mathbf{p}'; \mathbf{p}'', \mathbf{p}''') = -w_{s',s;s'',s'''}(\mathbf{p}', \mathbf{p}; \mathbf{p}'', \mathbf{p}''') =$$
$$= -w_{s,s';s''',s''}(\mathbf{p}, \mathbf{p}'; \mathbf{p}''', \mathbf{p}'').$$

For this reason we consider only the first equation of the system (17) in the following.

The equation for the symmetrical in spin indices solution ($x^{(1,\alpha)}_{0,\frac{1}{2}}(\mathbf{k},\mathbf{p}') = x^{(1,\alpha)}_{0,-\frac{1}{2}}(\mathbf{k},\mathbf{p}')$), has the form:

$$[\Omega_{\mathbf{p}} + \Omega_{\mathbf{k}-\mathbf{p}} - \lambda_\alpha(K)]x^{(1,\alpha)}_{0,\frac{1}{2}}(\mathbf{k},\mathbf{p}) +$$
$$+\frac{1}{4}\sum_{\mathbf{p}'}[w_{\frac{1}{2},-\frac{1}{2};-\frac{1}{2},\frac{1}{2}}(\mathbf{p},\mathbf{k}-\mathbf{p};\mathbf{k}-\mathbf{p}',\mathbf{p}') +$$
$$+w_{\frac{1}{2},-\frac{1}{2};\frac{1}{2},-\frac{1}{2}}(\mathbf{p},\mathbf{k}-\mathbf{p};\mathbf{k}-\mathbf{p}',\mathbf{p}')]x^{(1,\alpha)}_{0,\frac{1}{2}}(\mathbf{k},\mathbf{p}') = 0. \qquad (18)$$

Eqs.(16) and (18) describe the triplet states with different spin projection. It will be shown below that these equations are equivalent.

The equation for the antisymmetrical in spin indices solution to the system (17) ($x^{(0,\alpha)}_{0,\frac{1}{2}}(\mathbf{k},\mathbf{p}') = -x^{(0,\alpha)}_{0,-\frac{1}{2}}(\mathbf{k},\mathbf{p}')$) describes the singlet states:

$$[\Omega_{\mathbf{p}} + \Omega_{\mathbf{k}-\mathbf{p}} - \lambda_\alpha(K)]x^{(0,\alpha)}_{0,\frac{1}{2}}(\mathbf{k},\mathbf{p}) +$$
$$+\frac{1}{4}\sum_{\mathbf{p}'}[w_{\frac{1}{2},-\frac{1}{2};-\frac{1}{2},\frac{1}{2}}(\mathbf{p},\mathbf{k}-\mathbf{p};\mathbf{k}-\mathbf{p}',\mathbf{p}') -$$
$$-w_{\frac{1}{2},-\frac{1}{2};\frac{1}{2},-\frac{1}{2}}(\mathbf{p},\mathbf{k}-\mathbf{p};\mathbf{k}-\mathbf{p}',\mathbf{p}')]x^{(0,\alpha)}_{0,\frac{1}{2}}(\mathbf{k},\mathbf{p}') = 0. \qquad (19)$$

It is useful to express the interaction matrix $w$ in Eqs.(16),(18) and (19) in terms of the Hamiltonian parameters. In a more detailed form the Hamiltonian in the site representation may be written as:

$$H = \frac{1}{4}\sum_{mnm'n'} U^{(1)}_{mn,m'n'}c^+_{m,s}c^+_{n,s}c_{m',s}c_{n',s} + \qquad (20)$$
$$+\frac{1}{4}\sum_{mnm'n'} U^{(2)}_{mn,m'n'}(c^+_{m,s}c^+_{n,-s} + c^+_{m,-s}c^+_{n,s})(c_{m',s}c_{n',-s} + c_{m',-s}c_{n',s}) -$$
$$-\frac{1}{4}\sum_{mnm'n'} U^{(3)}_{mn,m'n'}(c^+_{m,s}c^+_{n,-s} - c^+_{m,-s}c^+_{n,s})(c_{m',s}c_{n',-s} - c_{m',-s}c_{n',s}),$$

where $s = 1/2$. The first two terms are responsible for the triplet interaction (matrices $U^{(1)}_{mn,m'n'}, U^{(2)}_{mn,m'n'}$ are antisymmetrical) whereas the third

term describes the singlet interaction (matrix $U^{(3)}_{mn,m'n'}$ is symmetrical). A comparison of the two equivalent expressions for the Hamiltonian (1), (21) gives:

$$U_{m,s;n,s;m',s;n',s} = U_{m,-s;n,-s;m',-s;n',-s} = U^{(1)}_{mn,m'n'};$$
$$U_{m,s;n,-s;m',s;n',-s} = U_{m,s;n,s;m',-s;n',s} = U^{(2)}_{mn,m'n'} - U^{(3)}_{mn,m'n'};$$
$$U_{m,s;n,-s;m',-s;n',s} = U_{m,-s;n,s;m',s;n',-s} = U^{(2)}_{mn,m'n'} + U^{(3)}_{mn,m'n'}. \quad (21)$$

Here the site and spin indices are shown separately for the sake of clarity. It seems reasonable to suppose that the form of the interaction depends only on the spin of a 4-fermion state, rather than on its spin projection. It leads to an equality $U^{(1)}_{mn,m'n'} = U^{(2)}_{mn,m'n'}$ , that, being not very important, makes calculations more easy. Using Eqs.(6), (12) in the momentum representation we may insert the Hamiltonian parameters (i.e. matrixes $U^{(1)}, U^{(2)}$ and $U^{(3)}$) into Eqs.(16),(18) and (19) instead of the function $w$. After some transformations one obtains the equation for the singlet states:

$$[\Omega_{\mathbf{p}} + \Omega_{\mathbf{k}-\mathbf{p}} - \lambda_{0,\alpha}(\mathbf{k})] x^{(0,\alpha)}_{0,s}(\mathbf{k},\mathbf{p}) + \quad (22)$$
$$+ \tfrac{1}{2}(th\tfrac{\beta\Omega_{\mathbf{p}}}{2} + th\tfrac{\beta\Omega_{\mathbf{k}\mathbf{p}}}{2}) \textstyle\sum_{\mathbf{p}'} U^{(3)}_{\mathbf{p},\mathbf{k}-\mathbf{p};\mathbf{k}-\mathbf{p}',\mathbf{p}'} x^{(0,\alpha)}_{0,s}(\mathbf{k},\mathbf{p}') = 0, \; s = \pm\tfrac{1}{2}.$$

Both of equivalent Eqs.(16), (18) for the triplet states may be transformed to:

$$[\Omega_{\mathbf{p}} + \Omega_{\mathbf{k}-\mathbf{p}} - \lambda_{1,\alpha}(\mathbf{k})] x^{(1,\alpha)}_{\sigma,s}(\mathbf{k},\mathbf{p}) + \quad (23)$$
$$+ \tfrac{1}{2}(th\tfrac{\beta\Omega_{\mathbf{p}}}{2} + th\tfrac{\beta\Omega_{\mathbf{k}\mathbf{p}}}{2}) \textstyle\sum_{\mathbf{p}'} U^{(1)}_{\mathbf{p},\mathbf{k}-\mathbf{p};\mathbf{k}-\mathbf{p}',\mathbf{p}'} x^{(1,\alpha)}_{\sigma,s}(\mathbf{k},\mathbf{p}') = 0, \; \sigma = 0, \pm 1.$$

Equations (22),(23) may be solved numerically though they are too complicated yet. As it will be shown below, the account of the finite number of sites in the interaction parameters $U^{(1)}, U^{(2)}, U^{(3)}$ permits to simplify the calculations significantly. An example of such a model is discussed in the next section.

## 2.3. Spectra of 2-particle excitations. 1 – 2 model

Let us fix up the form of the fermion – fermion interaction. It takes into account the interaction on the same or neighboring sites (1 – 2 model).

The interaction parameters $U^{(1)}, U^{(2)}, U^{(3)}$ (see expression (21)) in the momentum representation have the form:

$$U^{(1)}_{\mathbf{p},\mathbf{p}-\mathbf{k};\mathbf{k}'-\mathbf{p}',\mathbf{p}'} = U^{(2)}_{\mathbf{p},\mathbf{p}-\mathbf{k};\mathbf{k}'-\mathbf{p}',\mathbf{p}'} =$$
$$= \delta_{\mathbf{k}\mathbf{k}'} U_{t2} \sum_{\mathbf{l}} [cos(\mathbf{p}-\mathbf{p}',\mathbf{l}) - cos(\mathbf{k}-\mathbf{p}-\mathbf{p}',\mathbf{l})]$$
$$U^{(3)}_{\mathbf{p},\mathbf{p}-\mathbf{k};\mathbf{k}-\mathbf{p}',\mathbf{p}'} = \delta_{\mathbf{k}\mathbf{k}'}\{U_{s1} +$$
$$+U_{s2} \sum_{\mathbf{l}} [cos(\mathbf{p}-\mathbf{p}',\mathbf{l}) + cos(\mathbf{k}-\mathbf{p}-\mathbf{p}',\mathbf{l})]\},$$

where $U_{t2}$ is the interaction energy of the fermions in the triplet state and $U_{s2}, U_{s1}$ are the intersite and onsite interaction of the fermions in the singlet state; $\mathbf{l}$ is a lattice vector. Substituting these expressions into Eqs.(22, 23) one can obtain:

$$x^{(1,\alpha)}_{\sigma,s}(\mathbf{k},\mathbf{p}) - 2L_{kp}U_{t2} \textstyle\sum_{\mathbf{l}} sin(\frac{1}{2}\mathbf{k}-\mathbf{p},\mathbf{l}) \times$$
$$\times \textstyle\sum_{\mathbf{p}'} sin(\frac{1}{2}\mathbf{k}-\mathbf{p}',\mathbf{l}) x^{(1,\alpha)}_{\sigma,s}(\mathbf{k},\mathbf{p}') = 0 \qquad (24)$$

- for the triplet state and

$$x^{(0,\alpha)}_{0,s}(\mathbf{k},\mathbf{p}) - L_{kp} \textstyle\sum_{\mathbf{p}'}[U_{s1}$$
$$+2U_{s2} \textstyle\sum_{\mathbf{l}} cos(\frac{1}{2}\mathbf{k}-\mathbf{p},\mathbf{l}) cos(\frac{1}{2}\mathbf{k}-\mathbf{p}',\mathbf{l})] x^{(0,\alpha)}_{0,s}(\mathbf{k},\mathbf{p}') = 0 \qquad (25)$$

-for the singlet one. Here the notations are:

$$L_{kp} = \frac{1}{2}\frac{th(\beta\Omega_{\mathbf{p}}/2) + th(\beta\Omega_{\mathbf{k}-\mathbf{p}}/2)}{\lambda_{(\kappa,\alpha)}(\mathbf{k}) - \Omega_{\mathbf{p}} - \Omega_{\mathbf{k}-\mathbf{p}}},\ \Omega_{\mathbf{k}} = \omega_{\mathbf{k}} - \mu = t\sum_{\mathbf{l}} cos(\mathbf{k}\mathbf{l}) - \mu,$$

$\mathbf{p}$ is the internal momentum variable and the hopping integral is supposed to be $t(\mathbf{m}-\mathbf{n}) = t \neq 0$ only if $\mathbf{m} = \mathbf{n} \pm \mathbf{l}$. These equations obviously lead to the following $\mathbf{p}$ - dependence of the pair wave function:

$$x^{(1,\alpha)}_{\sigma,s}(\mathbf{k},\mathbf{p}) = L_{kp} \sum_{l=1}^{dim} A^{(t)}_l(\mathbf{k}) \sin(\frac{1}{2}\mathbf{k}-\mathbf{p},\mathbf{l}), \qquad (26)$$

$$x^{(0,\alpha)}_{0,s}(\mathbf{k},\mathbf{p}) = L_{kp}[A^{(s)}_0(\mathbf{k}) + \sum_{l=1}^{dim} A^{(s)}_l(\mathbf{k}) \cos(\frac{1}{2}\mathbf{k}-\mathbf{p},\mathbf{l})], \qquad (27)$$

where index $l = 1$ for $\mathbf{l} = (l_x, 0, 0)$, $l = 2$ for $\mathbf{l} = (0, l_y, 0)$, $l = 3$ for $\mathbf{l} = (0, 0, l_z)$ and *dim* stands for the dimensionality of the system. The lattice vector $\mathbf{l}$ numerates in a natural way the triplet bands and therefore the number of the triplet bands is equal to the space dimensionality. The coefficients $A_0^{(s)}(\mathbf{k}), A_l^{(s)}(\mathbf{k})$ $A_l^{(t)}(\mathbf{k})$ are determined by substitution of these functional forms into Eqs.(24, 25) for the wave functions. The equation describing the triplet pairs appears to be diagonal after this substitution and is transformed into linear independent algebraic equations for the functions $A_l^{(t)}(\mathbf{k})$:

$$[1 - 2U_{t2}H_l(\mathbf{k})]A_l^{(t)}(\mathbf{k}) = 0, l \leq dim$$

where $H_l = \sum_p L_{kp} \sin^2(\frac{1}{2}\mathbf{k} - \mathbf{p}, \mathbf{l})$. The excitation spectra are obtained from the equations:

$$1 - 2U_{t2}H_l(\mathbf{k}) = 0, \tag{28}$$

while the coefficients $A_l^{(t)}(\mathbf{k})$ are derived from the normalization condition (15) which is now written as $\sum_{p,s} x_{\sigma,s}^{(1,\alpha)*}(\mathbf{k}, \mathbf{p}) x_{\sigma,s}^{(1,\alpha')}(\mathbf{k}, \mathbf{p}) = \delta_{\alpha,\alpha'}$. With the account of Eq.(26) one obtains:

$$A_l^{(t)} = \left( \sum_p L_{kp}^2 \sin^2(\frac{1}{2}\mathbf{k} - \mathbf{p}, \mathbf{l}) \right)^{-1/2}.$$

As a result of the diagonalisation the triplet wave functions (26) appear to be rather simple:

$$x_{\sigma,s}^{(1,\alpha)}(\mathbf{k}, \mathbf{p}) = L_{k,p} A_l^{(t)}(\mathbf{k}) \sin(\frac{1}{2}\mathbf{k} - \mathbf{p}, \mathbf{l}). \tag{29}$$

The singlet pair case is more complicated. Nevertheless one can obtain a linear algebraic system of 4 equations on the coefficients $A_0^{(s)}(\mathbf{k}), A_l^{(s)}(\mathbf{k})$ by substituting expression (27) into Eq.(25):

$$(\hat{1} - \hat{M}) \begin{pmatrix} A_0 \\ A_1 \\ A_2 \\ A_3 \end{pmatrix} = 0, \tag{30}$$

where $\hat{M}$ is the matrix of rank 4:

$$\hat{M} = \begin{pmatrix} U_{s1}I_0 & U_{s1}I_1 & U_{s1}I_2 & U_{s1}I_3 \\ 2U_{s2}I_1 & 2U_{s2}I_{11} & 2U_{s2}I_{12} & 2U_{s2}I_{13} \\ 2U_{s2}I_2 & 2U_{s2}I_{21} & 2U_{s2}I_{22} & 2U_{s2}I_{23} \\ 2U_{s2}I_3 & 2U_{s2}I_{31} & 2U_{s2}I_{32} & 2U_{s2}I_{33}. \end{pmatrix} \tag{31}$$

and

$$I_0 = \sum_p L_{kp};\ I_l = \sum_p L_{kp}\cos(\tfrac{1}{2}\mathbf{k} - \mathbf{p}, \mathbf{l});$$
$$I_{lm} = \sum_p L_{kp}\cos(\tfrac{1}{2}\mathbf{k} - \mathbf{p}, \mathbf{l}) \cdot \cos(\tfrac{1}{2}\mathbf{k} - \mathbf{p}, \mathbf{m}).$$

The matrix $\hat{M}$ is written for the 3 – dimensional system. The same matrix for the 2 – dimensional system may be obtained by omitting the last column and the last line. For a 1 – dimensional system this simple procedure must be repeated. The spectra of the singlet states are found by equating the determinant of the system (30) to zero:

$$Det(\hat{1} - \hat{M}) = 0, \tag{32}$$

whereas the structure coefficients $A_0^{(s)}(\mathbf{k}), A_l^{(s)}(\mathbf{k})$ describing the wave function of the singlet pair (27) are found from Eq.(30) and the normalization condition:

$$\sum_{p,s} x_{0,s}^{(0,\alpha)}(\mathbf{k},\mathbf{p})^* x_{0,s}^{(0,\alpha')}(\mathbf{k},\mathbf{p}) = \delta_{\alpha,\alpha'}.$$

Now we have to find the excitation spectra of the local pairs by utilizing formulae (28) – (32). The numerical calculations have been done in the units: $D_{pol} = 4$. The results are represented in Fig.1 for the interaction value of $U_{s1} = +8$ (repulsive onsite interaction term); $U_{s2} = -6.8, U_{t2} = -6.5$ (attractive intersite terms for both the singlet and triplet states).

Here the most interesting case is considered: onsite repulsion (Coulomb force predominance) and intersite attraction. The concrete value of onsite repulsion has only a small effect on the character of band structure. The explanation is clear: two coupled fermions are placed on neighbor sites mostly where attraction dominates and "don't feel" onsite repulsion. On the contrary, the value of the intersite attraction is important for the determination of low – lying bands. This situation has been analysed in detail in [6]. The authors argued that the gap between the local pair band and

the polaron band, that is placed above, increases with the coupling constant when considering onsite attractive Hubbard model. The substitution of the onsite attraction by the intersite one does not affect this qualitative result. The choice of the attraction value $U_{s2} = -6.8$ is in agreement with experimental data on infrared absorbtion [21], neutron scattering [22] and gives reasonable mass of local pairs.

It becomes evident that the band structure is not as simple as in the standard 1-site attractive Hubbard model. There are additional gaps between the singlet and triplet bands, along with large ordinary one. Each of the singlet and triplet band in its own turn is splitted into two subbands. This may explain those contradictions that seem take place in determination of the gap value from different experiments. A one – particle (polaron) band is lying higher with the energy of its bottom being equal 2.0. It is necessary to normalize our relative units. As it will be shown below the experiments discussed in this paper can be fitted with the polaron bandwidth $D_{pol} = 19meV$ and the gap between the lowest bipolaron band and the bottom of the polaron one $\Delta = 10meV$ (see Fig.3). It means that our energy unit is about $5meV$ corresponding to the chosen value of the intersite attraction of $34meV (6.8 \cdot 5meV)$, that seems realistic.

Another interesting conclusion concerns a mass of the local pairs. According to the wide-spread point of view the local pair mass should be large enough this being considered as a shortcoming of local pair theories. Our calculations demonstrate (see Fig.1), that the situation is more favorable: the width of the lowest singlet band is only 3-4 times smaller, than the width of the fermion band. It gives the mass of the local pair $m^{**} \simeq 3 \div 4m^*$, where $m^*$ is the effective fermion mass. One can notice finally, that the triplet pairs appear to be several times heavier than the singlet ones for this set of parameters.

# 3. Local pairs in external fields

The excitation spectra and the local pair structure studied above may be used for theoretical investigation of thermodynamic and kinetic properties of the systems with the strongly interacting electrons. On the other hand there are many experiments dealing with the interaction of HTSC materials with different external fields. For the theoretical explanation of

these experiments one has to know the form of the interaction of the pairs with the external fields. The corresponding vertex functions should be obviously dependent on the internal structure of the coupled state. The interaction of the fermion with the external field presented in Eq.(1) for the Hamiltonian is of rather general form. It includes, for example, the interaction with neutrons and electromagnetic field. By integrating over the grassman variables in the same way as it was done before, one can obtain the action in the form (4), with the matrix $Y$ depending on the external field:

$$Y_{PP'} = \begin{pmatrix} Y_{11} & Y_{12} \\ Y_{21} & Y_{22} \end{pmatrix}, \tag{33}$$

$$Y_{11} = (r_{PP'} + i\epsilon\delta_{PP'})\delta_{\epsilon\epsilon'} + B(\epsilon - \epsilon')_{PP'},\ Y_{12} = \psi\left(\epsilon + \epsilon'\right)_{PP'},$$

$$Y_{21} = \psi^*\left(\epsilon + \epsilon'\right)_{PP'},\ Y_{22} - (r_{PP'} + i\epsilon\delta_{PP'})\delta_{\epsilon\epsilon'} - B(\epsilon - \epsilon')_{PP'}.$$

In Eq.(33) all matrices are written in the momentum representation and an imaginary "time" Fourier – transformation is assumed. Expanding this expression up to the second order in the fields $\psi, \psi^*$ and to the first order in the (weak) field $B$, one can obtain the effective action for the local pairs in the external field:

$$Z = \int DC^* DC \exp S(C^*, C),$$

$$S(C^*, C) = C_\sigma^{(\kappa\alpha)*}(\mathbf{k}, E)\,(iE - \lambda_{\kappa\alpha}(\mathbf{k}))\,C_\sigma^{(\kappa\alpha)}(\mathbf{k}, E) +$$
$$+ C_\sigma^{(\kappa\alpha)*}(\mathbf{k}, E)\,\Gamma_{\sigma\sigma'}^{(\kappa\alpha,\kappa'\alpha')}(\mathbf{k}, E, \mathbf{k}', E')\,C_{\sigma'}^{(\kappa'\alpha')}(\mathbf{k}', E').$$

Here the summation on the repeated indices is assumed. Eq.(14) and the orthonormal basis (13) were used in the derivation of this equation. The vertex $\Gamma$ has the form:

$$\Gamma_{\sigma\sigma'}^{(\kappa\alpha,\kappa'\alpha')}(\mathbf{k}, E, \mathbf{k}', E') =$$
$$= 2\sum_s B_{\sigma'-s,\sigma-s}(\mathbf{k} - \mathbf{k}', E - E')F_{\sigma\sigma's}^{(\kappa\alpha,\kappa'\alpha')}(\mathbf{k} - \mathbf{k}'). \tag{34}$$

Here the formfactor

$$F_{\sigma\sigma's}^{(\kappa\alpha,\kappa'\alpha')}(\mathbf{k} - \mathbf{k}') = \sum_{\mathbf{p}} x_{\sigma,\sigma-s}^{(\kappa,\alpha)*}(\mathbf{k}, \mathbf{k} - \mathbf{p}) x_{\sigma',\sigma'-s}^{(\kappa',\alpha')}(\mathbf{k}', \mathbf{k}' - \mathbf{p}), \tag{35}$$

depends only on the structure of the coupled state. The external field is written in the more convenient form – with the spin index extracted and translational invariance taken into account: $B_{PP'}(E) \equiv B_{s_p,s_{p'}}(\mathbf{p}-\mathbf{p}', E)$. As it was mentioned above, the vertex of the interaction of pairs with the external field depends on the frequency, the wave vector of the external field and the wave functions of the fermion pairs. One can see that the slowly varying field is not sensitive to the pair structure. A simple test shows that in this case the vertex of the singlet local pair interaction with the external field equals to zero. For the triplet pairs it is twice the interaction of the fermion with the field. The behavior of formfactor (35) plays a significant role in the theoretical explanation of experiments on the scattering of particles on the local pairs. For example, at low temperatures and small transferred momenta the transitions appear to be suppressed. The reason is quite obvious: at the low temperature the local pairs being bosons are condensed at the lowest level with the momenta $\mathbf{k} = 0$. The transitions into the upper bands with approximately the same momentum are suppressed due to the orthogonality of the wave functions with different energies: $F(\mathbf{k} - \mathbf{k}' = 0) = 0$.

The typical formfactors of the transitions from the lowest singlet band to the upper singlet or triplet one are presented in Fig.2. There is also the formfactor describing the transitions inside the lowest singlet band. The transitions into the second triplet band are forbidden for chosen transferred momenta $\mathbf{k} = (k_x, 0)$ due to the orthogonality of the wave functions. The evident momentum dependence of the formfactor confirms its importance in the interpretation of experiments.

# 4. Tunneling between bipolaron superconductor and a normal metal

The investigation of the tunneling through superconductor – normal metal junction provides an important information on the excitation spectra of superconductors. In the low – temperature superconductors accurate experiments confirmed unambiguously the BCS theory. Experiments on high – $T_c$ superconductors are much more complicated and far to be obvious for the explanation. There is no general consensus still on such important tunneling features, as the number of gaps in superconductors (one or

two [23, 24, 25, 26]); the existance of a smaller gap; the ratio $\frac{2\Delta}{kT_c}$ which varies from 0.7 to 2 – 12 in different experiments.

The main features of high – $T_c$ junction, which have been observed more or less firmly, are the presence of a large gap and the asymmetry of the tunneling current. A lot of experimental papers report on asymmetry, but its value varies from very small [25, 26, 27] to rather large [27, 28]. The observed temperature dependence of the gap is weak (if any) [25, 26]. The authors of paper [29] presented experimental data on the tunneling current with the asymmetry depending on the density of charge carriers. There are several papers that represent symmetrical conductivity curves [25, 27] as well.

The features mentioned above are not completely explained. Several theoretical models were suggested. First calculations on the basis of the local pair model [31] or bipolarons [32] led to a strongly asymmetrical tunnel conductance at low temperatures. To improve the situation and explain the asymmetry, the authors of the paper [31] supposed a smaller coupling interaction near junction than in the bulk material. In the paper [30] authors supposed the existence of local centers in high – $T_c$ material and obtained symmetrical curves, but they did not obtain any peaks in the $\frac{dI}{dV}$—$V$ characteristic. The authors of the paper [33] applied the idea of a local level and considered a potential barrier in the junction that contained localized electron states. In the framework of this model the low–energy gaplike structure and the experimentally observed two–gap behavior of the conductivity at low voltages was obtained. In Ref. [32] the tunnel current was studied in the framework of the bipolaron model. The existence of both large and small gaps and the origin of the asymmetry were explained there, but the theoretical tunneling conductance was too asymmetrical compared with the experimental one.

In this paper we propose a one-particle tunneling mechanism in the bipolaronic superconductors and explain several experimental features of the tunnel conductivity curves. We discuss here the simplest form of the model and neglect the tunneling of pairs because of the smallness of the two-particle tunnel probability comparing with that of one-particle. As it was predicted in the paper [32] and will be shown below, the accounting of the polaron band leads to a good agreement with the experiment. We considered as an example YBaCuO superconductor.

We investigate the tunneling through the superconductor – normal metal ($SN$) contact on the basis of the bipolaron theory of high – $T_c$ [32, 5]. We explain the asymmetry of the tunneling current, the mechanism of variation of its value from very small to an arbitrary large and weak temperature dependence of the experimental gap.

## 4.1. The tunneling mechanism

As it has been mentioned above, we choose the simplest form of tunnelling mechanism in the framework of the bipolaron model for high–$T_c$ superconductors [5]. There are two different mechanisms for tunneling of charge carriers: two–particle tunneling, discussed in Ref. [32] and one–particle tunneling. In this paper we consider the second one assuming that the first mechanism is exponentially suppressed. At positive voltage $V$ (Fig.3a) a process of tunneling consists of a bipolaron decay into an electron in a normal metal and a polaron in a polaron band of the superconductor. Evidently, this transition is allowed only at $V > \Delta$ ($T = 0, e = k_B = \hbar = 1$), where $\Delta$ is the gap between the bipolaron band and the polaron one. At the negative voltage $V < -\Delta$ the usual tunneling of the electrons into the polaron band takes place (Fig.3b). As one can see from Fig.3, tunneling mechanism is different at $V > 0$ and $V < 0$ which explains the tunnel current asymmetry. The effect of the polaron tunneling into a normal metal at positive voltage is negligible at low temperature when the polaron band is practically empty. Effects of upper bipolaron bands, such as triplet and $d$—wave [34] bands considered to be suppressed for the same reason. Two—particle tunneling from the upper band contributes only to a fine structure of the gap at a very small voltage. So, we suppose that different mechanisms are responsible for tunneling at different signs of voltage. To study these trasitions we use the standard tunneling Hamiltonian method [16], [35] and assume the Hamiltonian in the form:

$$H = H_S + H_N + H_T + V \sum_{\mathbf{k}} a^+_{\mathbf{k}} a_{\mathbf{k}}, \tag{36}$$

where $H_T$ is the Hamiltonian of the bipolaronic superconductor with a strong electron coupling, $H_N$ is the Hamiltonian of a normal metal.

The normal metal ($N$) is described by the Hamiltonian

$$H_N = \sum_{\mathbf{k}} \xi_{\mathbf{k}} a^+_{\mathbf{k}} a_{\mathbf{k}}, \tag{37}$$

where $a^+_{\mathbf{k}}, a_{\mathbf{k}}$, are the creation and annihilation operators for electrons in the normal metal, $\xi_{\mathbf{k}}$ is an electron energy. All energies are measured from a chemical potential level. The superconductor ($S$) assumed to be the material with bipolarons described by the bipolaronic Hamiltonian [5] as:

$$H_S = \sum_{\mathbf{p}} E_{\mathbf{p}} b^+_{\mathbf{p}} b_{\mathbf{p}} + \sum_{\mathbf{q}} \varepsilon_{\mathbf{q}} c^+_{\mathbf{q}} c_{\mathbf{q}}, \tag{38}$$

$b^+_{\mathbf{p}}$, $b_{\mathbf{p}}$ are creation and annihilation operators of bipolarons, $c^+_{\mathbf{q}}$, $c_{\mathbf{q}}$ are polaron operators, $E_{\mathbf{p}}$, $\varepsilon_{\mathbf{q}}$, are energy spectra of bosons and polarons respectively. As it follows from the previous discussion the tunneling Hamiltonian may be written in the form:

$$H_T = \frac{1}{\sqrt{N_1}} \sum_{\mathbf{p},\mathbf{q},\mathbf{k}} (D_{\mathbf{p},\mathbf{q},\mathbf{k}} b^+_{\mathbf{p}} c_{\mathbf{q}} a_{\mathbf{k}} + D^*_{\mathbf{p},\mathbf{q},\mathbf{k}\mathbf{p}} a^+_{\mathbf{k}} c^+_{\mathbf{q}}) +$$

$$+ \sum_{\mathbf{q},\mathbf{k}} (\mathcal{M}_{\mathbf{q},\mathbf{k}} c^+_{\mathbf{q}} a_{\mathbf{k}} + \mathcal{M}^*_{\mathbf{q},\mathbf{k}} a^+_{\mathbf{k}} c_{\mathbf{q}}), \tag{39}$$

where $D_{\mathbf{p},\mathbf{q},\mathbf{k}}$ is the matrix element of the bipolaron decay into a polaron (in the polaron band) and an electron (in the normal metal); $\mathcal{M}_{\mathbf{q},\mathbf{k}}$ is the matrix element of the electron transition into a polaron, $N_1$ is the number of cells in the superconductor. The determination of the tunneling matrix element is not simple problem, but as it will be pointed out in the next part, the main features of tunneling curves are independent of the form of the matrix element and we consider a simplest case, $D_{\mathbf{p},\mathbf{q},\mathbf{k}} = constant$ and $\mathcal{M}_{\mathbf{q},\mathbf{k}} = constant$.

## 4.2. The tunneling current

Our starting point is the calculation of the tunneling current using the standard method of the tunneling Hamiltonian [16], [35]:

$$< J >=< \frac{dN}{dt} >= -Im < [H_T, N] >, \tag{40}$$

where $< J >$ is the tunneling current , $< ... >$ means equilibrium state average. $N$ is the operator of number of particles in the normal metal. We choose the cubic cell units for the sake of simplicity. The calculation of the commutator (40) gives:

$$< J >= \frac{1}{\sqrt{N_1}} \sum_{\mathbf{p,q,k}} [D_{\mathbf{p,q,k}} < b_{\mathbf{p}}^{+} c_{\mathbf{q}} a_{\mathbf{k}} > - D_{\mathbf{p,q,k}}^{*} < b_{\mathbf{p}} a_{\mathbf{k}}^{+} c_{\mathbf{q}}^{+} >] - \tag{41}$$

$$- \sum_{\mathbf{q,k}} [\mathcal{M}_{\mathbf{q,k}} < c_{\mathbf{q}}^{+} a_{\mathbf{k}} > - \mathcal{M}_{\mathbf{q,k}}^{*} < a_{\mathbf{k}}^{+} c_{\mathbf{q}} >].$$

This expression may be written in the form:

$$< J >= 2Im[\frac{1}{\sqrt{N_1}} \sum_{\mathbf{p,q,k}} D_{\mathbf{p,q,k}} < b_{\mathbf{p}}^{+} c_{\mathbf{q}} a_{\mathbf{k}} > - \sum_{\mathbf{q,k}} \mathcal{M}_{\mathbf{q,k}} < c_{\mathbf{q}}^{+} a_{\mathbf{k}} >]. \tag{42}$$

The averages $< b_{\mathbf{p}}^{+} c_{\mathbf{q}} a_{\mathbf{k}} >$ and $< c_{\mathbf{q}}^{+} a_{\mathbf{k}} >$ are found from the following equations

$$\frac{d}{dt} < b_{\mathbf{p}}^{+} c_{\mathbf{q}} a_{\mathbf{k}} >= - < [H, b_{\mathbf{p}}^{+} c_{\mathbf{q}} a_{\mathbf{k}}] >$$

$$\frac{d}{dt} < c_{\mathbf{q}}^{+} a_{\mathbf{k}} >= - < [H, c_{\mathbf{q}}^{+} a_{\mathbf{k}}] >$$

and for the tunnel current we obtain:

$$< J >= 2Im \left[ \sum_{\mathbf{p,q,k}} \mid D_{\mathbf{p,q,k}} \mid^2 \frac{\varphi_{\mathbf{p}}(1 - f_{\mathbf{k}}^{(N)} - f_{\mathbf{q}}^{(pol)}) - f_{\mathbf{k}}^{(N)} f_{\mathbf{q}}^{(pol)}}{-E_{\mathbf{p}} + \varepsilon_{\mathbf{q}} + \xi_{\mathbf{k}} + V - i\delta} \right] - \tag{43}$$

$$- \sum_{\mathbf{q,k}} \mid \mathcal{M}_{\mathbf{q,k}} \mid^2 \frac{f_{\mathbf{k}}^{(N)} - f_{\mathbf{q}}^{(pol)}}{\varepsilon_{\mathbf{q}} - \xi_{\mathbf{k}} - V - i\delta} \Bigg]_{\delta \to 0} ,$$

$f_{\mathbf{k}}^{(N)} = f^{(N)}(\varepsilon_{\mathbf{k}})$ and $f_{\mathbf{q}}^{(pol)} = f^{(pol)}(\varepsilon_{\mathbf{q}})$ are Fermi distributions of electrons and polarons, $\varphi_{\mathbf{p}} = \varphi(E_{\mathbf{p}})$ is the Bose distribution of bipolarons, $\varphi_{\mathbf{p}} = n_0 \delta_{\mathbf{p,p_0}} + \varphi_{\mathbf{p}}^{'}$ , $n_0$ is the number of particles in the condensate at temperatures $T < T_c$. The spectra of particles are chosen in the forms $E_{\mathbf{p}} = \mathbf{p}^2/(2m_b)$, $\varepsilon_{\mathbf{q}} = \mathbf{q}^2/(2m_p) + \Delta$, $\xi_{\mathbf{k}} = \mathbf{k}^2/(2m_e) - E_F + \xi_0$, $\xi_0$ is the additional energy of the electrons in the normal metal. This energy shift usually appears when one connects two pieces of different crystals to make

their chemical potentials equal. We accounted this value using a condition $< J(V=0)=0 >$.

The second term in (43) describes the electron tunneling from the normal metal to the polaronic band and vice versa.

The first term describes the bipolaron decay. One of two electrons constituing a pair tunnels to the normal metal and the second goes to the polaron band simultaneously. At $T < T_c$ the charge conservation is provided partly by the bipolaron condensate motion with a momentum $\mathbf{p}_0 \neq 0$. The estimation of this momentum using the known values of the current leads to a small value of the boson energy $E_{\mathbf{p}_0} \leq 10^{-2} meV$ and may be neglected in the calculations. We assume $D_{\mathbf{p},\mathbf{q},\mathbf{k}} = D_0$, $\mathcal{M}_{\mathbf{q},\mathbf{k}} = \mathcal{M}_0$ for both matrix elements to simplify our calculations. The final expression for the tunnel current is:

$$< J >= A_0 \Bigg\{ \frac{\sqrt{2}\pi^2}{m_b^{3/2}} T^{3/2} \int_{\Delta/2T}^{(\Delta+D)/T} dx \sqrt{x-\Delta/T} \Big[ f^{(N)}(x - V/T - \xi_0/T) -$$

$$- f^{(pol)}(x) \Big] - \frac{\sqrt{2}\pi^2}{m_b^{3/2}} T^{3/2} \gamma \rho_0 \int_{\Delta/2T}^{(\Delta+D)/T} dx \sqrt{x-\Delta/T} \Big[ f^{(N)}(x + V/T +$$

$$+ \xi_0/T) - f^{(pol)}(x) \Big] - T^3 \gamma \int_0^{W/T} dx \sqrt{x} \int_{\Delta/2T}^{(\Delta+D)/T} dy \sqrt{y-\Delta/T} \cdot$$

$$\cdot \Big[ \varphi'(x) \Big( f^{(N)}(x + y + V/T + \xi_0/T) - f^{(pol)}(y) \Big) - \qquad (44)$$

$$- f^{(pol)}(y) f^{(N)}(-x - y - V/T - \xi_0/T) \Big] \Bigg\},$$

$$A_0 = \frac{2\sqrt{2} m_b^{3/2} m_p^{3/2} m_e^{3/2} |\mathcal{M}_0|^2 \sqrt{E_F} N_1 N_2}{\pi^6},$$

where $m_b, m_p, m_e$ are the masses of bipolarons, polarons and electrons in the normal metal respectively; $D = D_{pol}$ is the polaron bandwidth; $\gamma \equiv |D_0/\mathcal{M}_0|^2$, and $\rho_0$ is the number of particles per cell in the condensate. The first term in the expression (44) represents the 1-particle transitions between the polaron band and normal metal. The second term describes the decay and the transition of bipolarons in the condensate. The third term is the same one for supra-condensate bosons.

The density of the bosons in the condensate $\rho_0$ is calculated using the law of the particle conservation:

$$N = 2N_0^B + 2N_{\mathbf{p}\neq\mathbf{0}}^B + N^P,$$

$N$ is the number of charged fermions, $N_0^B$ is the number of bosons (bipolarons) in the condensate, $N^P$ is the number of particles in the polaron band, $N_{p\neq 0}^B$ is the number of the supra – condensate bosons. More detailed equation has the form

$$\rho_0 = \frac{\rho}{2} - \frac{\sqrt{2}m_b^{3/2}}{2\pi^2}\int_0^W dE[\sqrt{E}\varphi(E)] - \frac{\sqrt{2}m_p^{3/2}}{2\pi^2}\int_\Delta^{(\Delta+D)} d\varepsilon[\sqrt{\varepsilon-\Delta}f(\varepsilon)].$$

$\rho$ is the number of particles per cell, $\rho_0$ is the number of the condensate bosons per cell.

Let us compare now the values of the matrix elements $\mathcal{M}$ and $D$. Both of them contain matrix element of one – electron tunneling through junction that can be estimated in standard form [36]:

$$\mathcal{M} \sim \exp\{-\int\sqrt{2m_e(U-E)}\}dx \text{ and } D \sim \exp\{-\int\sqrt{2m_e(U-E')}\}dx.$$

Here $U$ is the potential of the barrier (the same for both matrix elements) and $E, E'$ are the energies of a tunneling electrons. Keeping in mind that $E - E' \sim \Delta \sim 10meV << U \sim 1eV$ we can put $\mathcal{M} \approx D$ and the value of $\gamma$ will be of the order unity. Of course, this is only an estimation and we consider $\gamma$ as a free parameter. As we will see below, the value $\gamma \sim 1$ does not contradict an experiment.

The main contribution into the expression (44) at $T \ll T_c$ is given by the first and the second terms, because of small number of supra–condensate bosons.

At $T = 0$ the expression can be calculated analytically and $< J >$ takes a form

$$< J >= A_0\frac{\sqrt{2}\pi^2}{m_b^{3/2}} \times \begin{cases} 0, & |V| < \Delta \\ \frac{2}{3}(V-\Delta)^{3/2}, & \Delta < V < \Delta + D \\ -\frac{2}{3}(|V|-\Delta)^{3/2}\rho_0\gamma, & \Delta < -V < \Delta + D \\ \frac{2}{3}(b-\Delta)^{3/2}, & V > \Delta + D \\ -\frac{2}{3}(b-\Delta)^{3/2}\rho_0\gamma, & V < -\Delta + D \end{cases}$$

and $\frac{dJ}{dV}$ is

$$\frac{dJ}{dV} = A_0 \frac{\sqrt{2}\pi^2}{m_b^{3/2}} \times \begin{cases} 0, & |V| < \Delta \\ (V-\Delta)^{1/2}, & \Delta < V < \Delta + D \\ (|V|-\Delta)^{1/2}\gamma\rho_0, & \Delta < -V < \Delta + D \\ 0, & |V| > \Delta + D. \end{cases} \tag{45}$$

We calculate also the tunnel current with the other form of the matrix element, $(NP)$ $\mathcal{M}_{qk} = \mathcal{M}_0\sqrt{q_x}$. This momentum dependence is well known in the case of the ordinary one-particle tunneling [16], [35]. The same result takes place for two-particle tunneling [32] as well. In this case the tunnel current has the following form at $T = 0$:

$$J = A_1 \times \begin{cases} 0, & |V| < \Delta \\ -\frac{2}{3}(|V|-\Delta)^{3/2}\gamma_1\rho_0, & \Delta < -V < \Delta + D \\ V^2/2 - V\Delta, & \Delta < V < \Delta + D \\ -\frac{2}{3}(b-\Delta)^{3/2}\gamma_1\rho_0, & V < -\Delta + D \\ b^2/2 - b\Delta, & V < \Delta + D, \end{cases} \tag{46}$$

where

$\gamma_1 = \sqrt{2}\pi|D|^2/(\sqrt{m_p}|\mathcal{M}_0|^2)$, $A_1 = 8\sqrt{2}m_p^2 m_c^{3/2}|\mathcal{M}_0|^2\sqrt{E_F}N_1N_2/(\pi^5)$

and the conductivity has the form:

$$\frac{dJ}{dV} = A_1 \times \begin{cases} 0, & |V| < \Delta \\ (|V|-\Delta)^{1/2}\gamma_1\rho_0, & \Delta < -V < \Delta + D \\ V - \Delta, & \Delta < V < \Delta + D \\ 0, & |V| > \Delta + D. \end{cases} \tag{47}$$

One can see by comparing the expressions (45) and (47), that the main features of the tunnel conductivity (the wide gap, the existence of two peaks and zero conductivity at high voltage) do not depend on the form of the matrix element.

Let us consider the results of numerical calculations of the tunneling current at the different parameters $\gamma$, $\rho$ and temperature $T$ using the formula (44). Temperature dependencies of the tunneling current are represented in Fig.4. One can see that, in spite of different mechanisms of tunneling at

$V > 0$ and $V < 0$, the temperature dependencies of the value of both peaks are similar at a wide range of temperatures. In Fig.4 we present the asymmetry of the curves for different values of the parameter $\gamma\rho$ (Fig.4a,4b). A slight variation of the charge carrier density $\rho$ or junction structure, that is represented by the parameter $\gamma$, leads to the alternation of the asymmetry. This might be a reason for the difference in the experimental results of Ref. [25] and of Ref. [26].

One can see from the inset in Fig.4a that the effective gap $\Delta_{eff}$ increasing with temperature decreasing. The physical explanation is obvious: the bosons leave the condensate and fill the upper levels of the boson band. It leads to the decreasing of the effective gap between the boson (bipolaron) and the fermion (polaron) bands.

The Fig.5 represents the comparison of our results with the experimental data. Fig. 5a is obtained with the parameter $\gamma\rho = 1.8$ and fits the experiment [27] at $|V/T_c| < 2$. The experimental asymmetrical tunneling current in Fig.5b was found in Ref. [27] as well. It may be fitted by our theoretical curve with the parameter $\gamma\rho = 1.28$. It is assumed that the junction structure varies for different samples that leads to the small variation of the parameter $\gamma\rho$. The behavior of the experimental curve at $|V/T_c| > 2$ is explained to our opinion by a phonon contribution that is considered in the next section.

## 4.3. The role of phonons

Our theoretical results are in a good agreement with experiments at low voltage and describe the gap features quite well. But as one can see in Fig.5 there is an essential difference behavior of the experimental and theoretical curves at high bias–voltage.

We have considered above the tunnelling processes where an absorbtion and emission of phonons were neglected. It will be shown here that the phonons considerably improves our fit. We keep in mind that only emission is essential at low temperatures. Here only one-phonon emission is taken into account. A momentum dependence of the phonon energy is neglected too. The calculation leads to the tunneling current of the form,

$$J = J_0 + J_1. \tag{48}$$

Here $J_0$ is the expression (44), and $J_1$ is the one-phonon contribution

$$< J_1 >= zA_0\{\frac{\sqrt{2}\pi^2}{m_b^{3/2}}T^{3/2}\int_{\Delta/T}^{\Delta+D)/T} dx\sqrt{x-\Delta/T}\cdot \qquad (49)$$

$$\cdot[f^{(N)}(x-V/T-\xi_0/T-\omega/T)-f^{(pol)}(x)]-$$

$$-\frac{\sqrt{2}\pi^2}{m_b^{3/2}}T^{3/2}\gamma\rho_0\int_{\Delta/T}^{\Delta+D)/T} dx\sqrt{x-\Delta/T}\left[f^{(N)}(x+V/T+\xi_0/T+\omega/T)q-\right.$$

$$-f^{(pol)}(x)-T^3\gamma\int_0^{W/T} dx\sqrt{x}\int_{\Delta/T}^{\Delta+D)/T} dy\sqrt{y-\Delta/T}\cdot$$

$$\cdot[\varphi(x)\left(f^{(N)}(x+y+V/T+\xi_0/T+\omega/T)-f^{(pol)}(y)\right)-$$

$$-f^{(pol)}(y)f^{(N)}(-x-y-V/T-\xi_0/T-\omega/T)]\},$$

$z$ is the multyplaer that contains the constant of the electron-phonon interaction.

The expression (48) for $T \neq 0$, calculated numerically at arbitrary temperature, is shown in Fig.6. It becomes evident that the phonon radiation is responsible for the behavior of the tunneling current at high voltage. The phonon radiation increases effectively the width of the peaks and does not influence the gap width. Similar phonon structure has been observed in the experiment that was described in paper [37].

The bipolaron model [5] appears to be able to explain the main experimental features of the tunneling current. The mechanism of the tunneling current consists of the bipolaron decay to the polaron in the superconductor and the electron in the metal. This model explains the experimental value of the gap, the form of the gap peak, the different value of the asymmetry in different tunnel experiments. The temperature dependence of the gap is one of the hallmarks of the BCS theory. Our result on the temperature dependence of the gap width is shown in the inset of Fig.4. This curve is not similar to that of the BCS theory.

Taking into account of the phonon emission even in the simplest form improves the agreement with the experiment at high voltage.

# 5. Neutron scattering

There are several experiments with superconducting $YBa_2Cu_3O_{6+x}$, where the intensity of scattered neutrons has been measured very accurately at low temperatures. The main, still unexplained feature of the neutron intensity is its nontrivial behavior near the center of Brilluen zone. We show in this section that bipolaron theory explains rather good this feature. The energy and temperature dependencies of intensity as well as sinusoidal modulation of neutron intensity in c-direction are considered. We discuss also the reason of noticeable decreasing of the neutron intensity above critical temperature $T_c$.

The interaction of electrons with an arbitrary external field (1) causes the complex interaction of bipolarons with the external field. As was shown in third section, the vertex is dependent on the bipolaron wave function structure. More general expression of the Action incorporating the triplet states has the form:

$$S_I = \sum b_\sigma^{(\alpha)*}(E,\mathbf{k})\Gamma_{\sigma,\sigma'}^{(\alpha,\alpha')}(E-E',\mathbf{k},\mathbf{k}')b_{\sigma'}^{(\alpha')}(E',\mathbf{k}'), \qquad (50)$$

$$\Gamma_{\sigma,\sigma'}^{(\alpha,\alpha')}(E-E',\mathbf{k},\mathbf{k}') = 2\sum_{s,\mathbf{p}} B_{\sigma'-s,\sigma-s}(E-E',\mathbf{k},\mathbf{k}')x_{\sigma,s}^{(\alpha)*}(\mathbf{k},\mathbf{p})x_{\sigma',s}^{(\alpha')}(\mathbf{k}',\mathbf{p}),$$

where $x_{0,s}^{(\alpha)}(\mathbf{k},\mathbf{p}) = u^{(\alpha)}(\mathbf{k},\mathbf{p})$ is the wave function of the singlet bipolaron, $x_{\sigma,s}^{(\alpha)}(\mathbf{k},\mathbf{p})$ is that of the triplet bipolaron, $s = \pm 1/2$ is a spin projection of an electron in the coupled state, $\sigma = \pm 1$ is the spin projection of the bipolaron, $b_\sigma^{(\alpha)*}(E,\mathbf{k})$ is the creation operator of the bipolaron with spin projection $\sigma = 0, \pm 1$, energy E and momentum $\mathbf{k}$ at the band $\alpha$, $x_{\sigma,s}^{(\alpha)*}(\mathbf{k},\mathbf{p})$ is bipolaron wave function. The expression (50) is quite general and may be used not only in the particular case of the neutron scattering. We propose the original neutron - electron interaction is described by the vertex:

$$H_{ne} = \sum \lambda_{s_p - s_q} C_{s_{p'}\mathbf{p}'}^{+} C_{s_{q'}\mathbf{q}'} a_{s_p\mathbf{p}}^{+} a_{s_q\mathbf{q}} \delta(\mathbf{p}+\mathbf{p}'-\mathbf{q}-\mathbf{q}')\delta(s_p+s_{p'}-s_q-s_{q'}).$$

Here $C_{s_q\mathbf{q}}^{+}, C_{s_q\mathbf{q}}$ are the creation and annihilation operators of neutron with spin $s_q$ and momentum $q$. Considering the expression

$$\lambda_{s_p - s_q} C_{s_{p'}\mathbf{p}'}^{+} C_{s_{q'}\mathbf{q}'} \delta(\mathbf{p}+\mathbf{p}'-\mathbf{q}-\mathbf{q}')\delta(s_p+s_{p'}-s_q-s_{q'})$$

as the special case of external field in the momentum representation, we obtain the part of the Action responding to neutron-bipolaron interaction from Eqs(50) in the form:

$$S_I = 2\sum \lambda_{s_p - s_q} F^{(\alpha,\alpha')}_{\sigma,\sigma'}(\mathbf{k},\mathbf{k}')\delta(\mathbf{p}-\mathbf{p}'+\mathbf{k}-\mathbf{k}')\delta(s-s'+\sigma-\sigma')$$
$$\delta(E-E'+\varepsilon-\varepsilon')b^{(\alpha)*}_{\sigma}(E,\mathbf{k})b^{(\alpha')*}_{\sigma'}(E',\mathbf{k}')C^{+}_{s}(\varepsilon,\mathbf{p})C_{s'}(\varepsilon',\mathbf{p}'), \tag{51}$$

where the vertex $F^{(\alpha,\alpha')}_{\sigma,\sigma'}(\mathbf{k},\mathbf{k}')$ includes the wave functions structure:

$$F^{(\alpha,\alpha')}_{\sigma,\sigma'}(\mathbf{k},\mathbf{k}') = \sum_{s,\mathbf{p}} x^{(\alpha)*}_{\sigma,s}(\mathbf{k},\mathbf{p})x^{(\alpha')}_{\sigma',s}(\mathbf{k}',\mathbf{p}). \tag{52}$$

## 5.1. Neutron intensity calculation

The main peak of the neutron intensity at approximately $40-41meV$ can be explained by the neutrons scattering on the bipolarons with consequent decay of the last into two polarons. The experiments discussed above were carried out at definite energy and momentum transfer. The well known formula for neutron intensity [38] is transformed into:

$$I = \frac{dw}{dq_c dq_{ab} d\omega} = const \frac{q_{ab}}{\sqrt{q_{ab}^2 n_{ab}^2 - [m_n\omega + q^2/2 - q_c n_c]^2}} \cdot$$
$$\cdot \int d^2k d^2p_1 d^2p_2 F^2(\mathbf{q}_{ab}) n_B(E_k)[1-n_F(\varepsilon_{p_1})][1-n_F(\varepsilon_{p_2})] \cdot$$
$$\cdot \delta(\mathbf{k}+\mathbf{q}-\mathbf{p}_1-\mathbf{p}_2)\delta(E_k+\omega-\varepsilon_{p_1}-\varepsilon_{p_2}), \tag{53}$$

where the expression (51) is used for calculation of the matrix element. The multiplier arises due to variable exchange $d\Omega \rightarrow dq_{ab}dq_c$. Here we denote $\mathbf{q}_c$ and $\mathbf{q}_{ab}$ are momentum transfer parallel to and perpendicular to $c$-axis, $\omega$ is the energy transfer, $dw$ is the probability of the neutron scattering with definite energy and momentum transfer $\mathbf{n}$ is the neutron momentum, $m_n$ is its mass, $E_k, \mathbf{k}$ are the energy and momentum of initial bipolarons, $\varepsilon_{p_1}, \varepsilon_{p_2}$ and $\mathbf{p}_1, \mathbf{p}_2$ are the energies and the momenta of final polarons, $n_B$and $n_F$ are Bose- and Fermi- distributions. Formfactor $F$ of transition from the lowest bipolaron band into the polaron one has been calculated as discussed in previous section:

$$F(\mathbf{q}) = \sin q_x/2 \cdot \sin(k_x'/2 - p_x - q_x/2) + \sin q_y/2 \cdot \sin(k_y'/2 - p_y - q_y/2)$$

The polaron spectrum is supposed to be

$$\varepsilon_p = \Delta + (D-D')(2-\cos p_x - \cos p_y) + D'(2-\cos(p_x+p_y) - \cos(p_x-p_y),$$

The last term corresponds to next-nearest neighbor hopping [39] and supposed to be a small correction ($D' << D$).

The results of numerical calculations of $\mathbf{q}_{ab}$ and $\omega$ dependencies at temperature T=0 are represented in Fig.7 and 8. The peak at the 2d-zone center (Fig.7) is explained quite easily keeping in mind the form of the formfactor $F(\mathbf{q})$. Indeed, there are only singlet pairs with zero momentum at T=0 and we have $\mathbf{k} = 0$. The analysis of the expression for the formfactor indicates its monotonous increasing with momentum transfer up to the zone center $\mathbf{q} = (\pi, \pi)$.

The polaron bandwidth $D$ and the gap $\Delta$ between lowest bipolaron band and polaron one are responsible to the position of the wide maximum in Fig.7. Here the values of the parameters appear to be: $D = 19meV, \Delta = 10meV$ in good agreement with that extracted from tunnel experiments [40, 41].

The width of the calculated peak is determined by the single fitting parameter $D'$. One can note however, that the experimental width depends on several effects, such as phonon emission, experimental inaccuracy in energy measurement, secondary scattering of the neutrons in crystal and so on. As a result, the value of the parameter $D'$ may be changed significantly and obtained value should be considered as its maximum value.

The temperature dependency are shown in the Fig.9. Evidently, the evaporation of the bipolaron condensate with temperature is responsible to intensity decreasing. The effect above $T_c$ exists, but small enough to be detected. The coincidence with experimental results [42] is rather good.

The bipolaron transitions into upper bipolaron bands are responsible to the neutron scattering at less energies [43]. Their intensity are small in comparison with the peak at 41 meV for 2-particle phase volume in the final state (neutron + bipolaron) is small in comparison with 3-particle one (neutron + two polarons).

The dependence of the neutron intensity on oxygen concentration can be understood in the basis of our model if one notes that oxygen doping changes the crystal structure and hence the polaron interaction energy. It change in its turn the bipolaron band structure discussed above.

Magnetic susceptibility is proportional to the square of the matrix element in question. It is usually considered proportional to neutron intensity at

$T = 0$ as well, supposing the phase volume being constant. Here we see that this is not the case, though essential features of the neutron intensity are preserved in an expression for magnetic susceptibility.

## 5.2. $Q_c$ dependence of neutron intensity

Till now we were dealing with q-dependence in '$a - b'$ plane, where cells are practically square and we are able to use our model for the calculating of the wave function structures and neutron intensity. The calculation of the intensity as a function of momentum transfer in c- direction is more difficult problem, because we have to include the second Cu-O plane into consideration. But we will show here that only a supposition on bipolarons existence allows to explain the experimental behavior of neutron intensity. The experiment [43], [44] shows the sinusoidal modulation of intensity and slow decreasing of the amplitude with momentum transfers $q_c$ normal to the CuO planes.

Let us suppose a bipolaron, being placed in the definite CuO plane (z=0), has the wave function $\phi(z)$ with narrow maximum at z=0 (only z argument of function will be discussed further). Because the hopping between CuO plane is suppressed, the influence of the neighbor CuO plane consists of splitting the level. Now we have two levels in the states:

$$\Phi_{s,a}(z) = \frac{1}{\sqrt{2}}[\phi(z) \pm \phi(z + z^*)],$$

where $z^*$ is the distance between adjacent CuO planes.

We have shown in this section that there exist another bipolaron states. Denote the lowest singlet state as $\phi(z)$ and triplet state as $\psi(z)$ . The triplet states splitted also:

$$\Psi_{s,a}(z) = \frac{1}{\sqrt{2}}[\psi(z) \pm \psi(z + z^*)],$$

Now we are able to write the amplitude of neutron scattering with spin

flipping. There are two channels :

$$A_{s,a} = const \int dz \Psi_{s,a}(z) e^{i(n_c - k_c)z} \Phi_s^*(z) \qquad (54)$$

Here the wave function of neutron with momentum '$n$' is proportional to $e^{in_c z}$. The (54) may be easily simplified due to the supposed sharpness of the functions $\phi(z)$ and $\psi(z)$. The final expression for symmetrical final state transition has the form:

$$A_s = g_s e^{iq_c z^*} J(q_c) \cos(q_c z^*/2),$$

$$J(q_c) = \int dz e^{iq_c z} \phi(z) \psi^*(z) \qquad (55)$$

where $q_c = n_c - k_c$. The transition into antisymmetric final state may be obtained also:

$$A_a = i g_a e^{iq_c z^*} J(q_c) \sin(q_c z^*/2).$$

It is reasonable to suppose that the unknown parameters $g_a, g_s$ are obey a relation $g_a \sim 3g_s$ due to statistical weight of a triplet state.

The intensity of scattered neutrons is proportional to the expression:

$$I = \mid A_s \mid^2 + \mid A_a \mid^2 = (g_a)^2 J^2(q_c)[\xi + (1-\xi)\sin^2(q_c z^*/2)], \qquad (56)$$
$$\xi = (g_a/g_a)^2 \sim 0.1$$

with exactly the same period of oscillations, that was found experimentally.

One can note that previous consideration is valid for pairs of itinerant electrons (polarons) in the polaron band.

The additional prediction of our model concerns the behavior of the neutron intensity amplitude (56) with momentum. Evidently the factor $J(q_c \to 0) \to 0$ tends to zero due to the orthogonality of wave functions and $J(q_c \to \infty) \to 0$ due to the oscillateing function in the integrand of expression (55).

# 6. Infra-red absorption spectra

Investigation of optical spectra of high - $T_c$ superconductors in a far infrared region (IR) makes it possibble to obtain important information about a superconducting gap as well as about band structure above threshold energy. Explanation of properties of optical spectra observed in IR region is not complete inspite of a great number of publications on this problem. Analysis of experimental results made in review [46] and investigations in [21], [47] permits to draw a conclusion that at low temperatures ($T \approx 10K$) YBaCuO metal oxides have a frequency region ($\nu < 100cm^{-1}$) in $E \perp C$ polarization where there is no any absorption. In some cases the absorption age is stepwise. The properties of the absorbtion spectra are detected also at larger frequencies with their position well correlated with the energy of some optical phonons. It is known also that frequency dependence of conductivity is not described by Drude model [46].

The aim of this section is to explain the IR spectra features mentioned above on the basis of the bipolaron [5], [18], [17] model. The imaginary part of a dielectric susceptibility has been considered at low frequencies. Theoretical calculations are compared with the experiment - [46], [21], [47].

## 6.1. Stepwise properties of imaginary part of dielectric susceptibility in $E \perp C$ polarization

Let us consider photon absorption in the system described above at $T = 0$. In the bipolaron framework the process of absorption includes bipolarons transitions from the ground state (with zero quasimomentum) into excited states. Transitions into the polaron band are suppressed, since we consider the energy of infrared photon to be less than the gap between the ground state and the polaron band. Direct transitions into the low lying boson (bipolaron) bands are suppressed as well. Indeed, as we shall see below, a matrix element to be proportional to the formfactor that in its turn contains momentum of a photon as an argument. The photon momentum is almost zero and hence the formfactor is small too, as one can see from Fig.2. Transitions into other bands appear to be essential if radiation of optical phonons is taken into account (nondirect transitions). Let us consider only that part of Hamiltonian, which is responsible for the process

in question at a low temperature:

$$H_2 = g_{e-m} \sum_{\mathbf{p},\mathbf{q},\sigma} A_{\mathbf{p}-\mathbf{q}}(t) c^+_{\mathbf{p},\sigma}(t) c_{\mathbf{q},\sigma}(t) +$$

$$+ g_{phonon} \sum_{\mathbf{p},\mathbf{q},\sigma} d_{\mathbf{p}-\mathbf{q}} c^+_{\mathbf{p},\sigma}(t) c_{\mathbf{q},\sigma}(t) + h.c. \qquad (57)$$

Here $c, c^+$ are operators of annihilation and creation of fermions, $d$ is an annihilation operator of phonons, and $A$ is an annihilation operator of photons with the polarisation perpendicular to $C$ axis.

Comparison of the expressions (1) and (57) leads to the following form of the external field $B_{PQ}$:

$$B_{PQ}(t) = g_{e-m} A_{\mathbf{p}-\mathbf{q}}(t) \delta_{\sigma_P,\sigma_Q} + g_{phonon} d_{\mathbf{p}-\mathbf{q}}(t) \delta_{\sigma_P,\sigma_Q}.$$

To obtain an effective Hamiltonian in terms of the local pairs, we have to expand the effective Action in expression (2) from the paper [18] up to the second power of the field $B_{PQ}$. Taking into account only the term with both phonon and photon operators along with bipolaron creation and annihilation operators one obtains the effective interaction vertex:

$$H_{int} = \lambda \sum_{\mathbf{k},\mathbf{k}',\mathbf{p},\mathbf{p}'} F\left(\mathbf{k}-\mathbf{k}'\right) b^+_{\mathbf{k}}(t) b_{\mathbf{k}'}(t) d^+_{\mathbf{p}}(t) A_{\mathbf{q}}(t) \delta(\mathbf{k}'+\mathbf{p}-\mathbf{k}-\mathbf{q}) + h.c. \qquad (58)$$

where $\lambda \sim g_{e-m} \cdot g_{phonon}$, $F(\mathbf{k}-\mathbf{k}')$ - is the form-factor that was calculated in part 3 (see Fig.2). Here we suppose $\lambda$ being constant at a small transferred quasimomentum and energy.

The transition probability of the bosons (bipolarons) from the ground state into singlet band with quasimomentum $\mathbf{k}$ and energy $E^b(\mathbf{k})$ can be written using the perturbation theory:

$$P_{0\to k} = 2\pi \mid \langle \mathbf{k}, \mathbf{p} \mid H_{int} \mid in \rangle \mid^2 \delta\left(E^b(\mathbf{k}) + E^{ph}(\mathbf{p}) - \omega\right). \qquad (59)$$

Here $E^{ph}(\mathbf{p}), \mathbf{p}$ are energy and quasimomentum of radiated phonon. The photon momentum is small as usual and is assumed to be equal to zero (q=0). The initial state $\mid in\rangle$ includes a photon with the energy $\omega$ and a bipolaron in the lowest band with zero quasimomentum. The latter is justified at a zero temperature. The final state $< \mathbf{k}, \mathbf{p} \mid$ describes the

bipolaron and the phonon with quasimomenta $\mathbf{k}, \mathbf{p}$ respectively. Note that quasimomentum conservation results in a simple equality $\mathbf{p} = -\mathbf{k}$. The transitions are considered at a zero temperature, hence the bipolarons are in condensate and the matrix element in (59) is proportional to the condensate density $\sqrt{N_0}$. The transition probability and the density of the absorpted energy per second are connected by a well-known equality $Q = \frac{\omega}{V}\sum_{\mathbf{k}} P_{0\to k}$. Consequently, the imaginary part of dielectric susceptibility $\varepsilon_2(\omega)$ can be expressed in the form $\varepsilon_2(\omega) = \frac{4\pi}{E_m^2\omega}Q$ [48] and, finally:

$$\varepsilon_2(\omega) = \frac{N_0}{\omega}\sum_{\mathbf{k}} F^2(\mathbf{k})\,\delta\left(E^b(\mathbf{k}) + E^{ph}(-\mathbf{k}) - \omega\right), \tag{60}$$

where $E_m$ is an amplitude of an electromagnetic wave. It is easy to see by comparing formfactors in Fig.2, that the contribution in expression (60) from the top band is less than that of the lowest band and can be omitted. For the sake of simplicity we shall neglect also the interaction of the bosons that are situated in neighboring planes and consider 2D space that is supposed to be isotropic. To obtain the result in an analytical form we accept approximations for the formfactor form and for the energy spectrum:

$$E^b(k) = E^b(\pi)\sin(k/2) \tag{61}$$

$$F(k) = \frac{1}{2}[F(0) + F(\pi) + (F(0) - F(\pi))\cos(k)]. \tag{62}$$

It is taken into account in approximation (61) that the boson spectrum at small quasimomenta is linear at a temperature below the critical one. The dispersion law for phonons is written in the form (according to [49], the phonon of such material has a quasi-2D character):

$$E_i^{ph}(k) = \frac{1}{2}[E_i^{ph}(0) + E_i^{ph}(\pi) + (E_i^{ph}(0) - E_i^{ph}(\pi))\cos(k)], \tag{63}$$

where the subscript $i$ denotes a few branches of optical phonons. As a result we obtain:

$$\epsilon_2 = \frac{const}{\omega}\int_0^{\pi} kF^2(k)\,\delta\left(E^b(k) + E^{ph}(k) - \omega\right)dk. \tag{64}$$

Let us denote the argument of delta-function as $G$ and taking into account (61), (63) one can transform it into the form:

$$G(\xi) = E^b(\pi)\xi + \frac{1}{2}[E_i^{ph}(0) + E_i^{ph}(\pi) + (E_i^{ph}(0) - E_i^{ph}(\pi))(1 - 2\xi^2)] - \omega, \tag{65}$$

where $\xi = E^b(k)/E^b(\pi)$. Inserting approximations (61)-(63) into expression (64) and integrating out $\delta$-function we obtain:

$$\epsilon_2 = \frac{const}{\omega} \sum_{i=1}^{n} \sum_{j=1}^{m} \arcsin(\xi_j) \cdot \cdot \frac{\left[F(0)+F(\pi)+(F(0)-F(\pi))\left(1-2\xi_j^2\right)\right]^2}{\left|2(E_i^{ph}(0)-E_i^{ph}(\pi))\xi_j - E^b(\pi)\right|\left(1-\xi_j^2\right)^{1/2}}, \quad (66)$$

where

$$\xi_{1,2}(\omega) = \frac{E^b(\pi)}{2(E_i^{ph}(0)-E_i^{ph}(\pi))} \pm \pm\sqrt{\left(\frac{E^b(\pi)}{2(E_i^{ph}(0)-E_i^{ph}(\pi))}\right)^2 - \frac{\omega - E_i^{ph}(0)}{E_i^{ph}(0)-E_i^{ph}(\pi)}} \quad (67)$$

are the roots of the equation $G(\xi) = 0$, that is the law of energy conservation. Previous analysis is needed ( see Appendix ) before the substitution of Eq.(67) in Eq.(66). Clearly, expression (67) has the pole at the photon energy $\omega^* = E_i^{ph}(\pi) + E^b(\pi)$ along with the density of states having the pole at $k = \pi$. This pole can be observed as sharp peak in experimental curves. The position of the peak is determined by dispersion of both phonons and bipolarons. Indeed, let us consider quasimomentum dependence of the total energy of the final state $E_{tot}(\mathbf{k}) = E_i^{ph}(\mathbf{k}) + E^b(\mathbf{k})$ (Fig.10). Remind that an absolute value of quasimomenta of phonons and bipolarons are equal in the final state. Scattering takes place if the photon energy $\omega > E_{tot}$. There are two different cases:

a. The dispersion of optical phonons is larger than the lowest bipolaron bandwidth. This case is represented by curve 1 in Fig.10. The photon energy threshold $\omega_{th} = E_i^{ph}(\pi) + E^b(\pi)$ is equal to the pole ($\omega_{th} = \omega^*$) of expression (67). This explains the coincidence of singularity and threshold positions. The process of this type was observed experimentally to be stepwise on $YBa_2Cu_3O_{6,8}$ sample in the paper [21] (Fig.11a).

b. The dispersion of optical phonons is small. In this case, although the threshold of the reaction exists, the narrow peak that corresponds to the pole of expression (67) is inside the allowed region. The process of the second type has been investigated on $YBa_2Cu_3O_{6,9}$ sample in the paper [47]. There are other papers (see for example [49] and references therein) with the data on the IR-absorption which we classify here as second type prosseses.

As it will be shown below the first prosses is realized under the condition $\rho \equiv (E_i^{ph}(0) - E_i^{ph}(\pi))/E^b(\pi)) > 1$, while the second - at $\rho < 1$. The parameter $\rho$ can not be determined experimentally for phonon dispersion has been studied unsufficiently in YBaCuO - materials and this parameter remains arbitrary. We analyze below various data on phonon spectra and point out the phonon branches that contribute to the absorption. In our case the polarization of photons and quasymomenta of phonons are perpendicular to axis $C$. Therefore only longitudinal modes ($LO$-phonons) propagating in a basic plane can be excited. As it follows from the analysis that was carried out in [49], optical oscillations can be separated into two classes. The first is the class of low-frequency modes ($\nu < 200cm^{-1}$). These modes are connected with interlayer oscillations of heavy cations. Such layers can be situated along the basic plane as well as perpendicularly to it. This class is characterized by appreciable dispersion in any direction of Brillouin zone. The second class modes are connected with intralayer oscillations of oxygen atoms. These high frequency modes ($\nu > 200cm^{-1}$) can be excluded from the consideration for their energies are large in comparison with the energies in question. Therefore, at the frequencies $\nu < 200cm^{-1}$ we should take into account the bosons as well as the low-frequency phonons connected with interlayer oscilations. The position of the singularity in the absorption spectrum ought to correlate with the energy of such phonons. Low $LO$-modes that belong to $B_{1u}$ and $A_g$ symmetries satisfy this conditions.

Using data about IR-TO-mode of $B_{1u}$ symmetry and taking into account the fact that $TO - LO$-splitting is small [21] we choose a numerical value $E_1^{ph}(0) = 14,0meV$. The begining of the second phonon branch is chosen as $E_2^{ph}(0) = 18,8meV$. This branch corresponds to $A_g$ symmetry and it was obtained from Raman scattering [50]. As it was mentioned, the edges of the phonon spectra were studied insufficiently. Therefore the values of phonon dispertions were not determined accurately and one has to use fit parameters. We show below that the experiments can be explained with only one free parameter. The spectra of local pairs shown in Fig.1 are in agreement with the experimental data on low energy neutron scattering [43] in $YBaCuO$. The results of numerical calculations of the dielectric susceptability $\epsilon_2(\omega)$ are shown in Fig. 11b (energy is expressed in units - $cm^{-1}$, where $1,0meV = 8,1cm^{-1}$). Fig. 11a represents the experimetal data given in [21] on the $YBa_2Cu_3O_{6.8}$ sample at $T = 10K$ ($T_c = 80K$) and $E \perp c$. Assuming that the dispersions of both phonon branches were

equal to $2.8meV$ one can obtain that $E_1^{ph}(\pi) = 11.2meV$ and $E_2^{ph}(\pi) = 16.0meV$.

The theoretical dependence in Fig. 11b was obtained taking into account the formfactor in Fig.2: $F(0) = 1$; $F(\pi) = 0.7$. As it follows from Fig. 11 there is a good agreement between experimental data and our calculations. The second sharp peak is determined by the second optical branch. It is necessary to note that the free parameter of the phonon dispersion (=2.8 meV) provides the condition $\rho > 0$. It seems natural, that interlayer modes are very sensitive to the change of a lattice structure, in particular to an interlayer distance. It is well-known that the bridge atom of oxygen 04 is an important element for the formation of an interlayer coupling, but it is not available such a nonsupercoducting structure as $YBa_2Cu_3O_6$. We come to a conclusion that oxygen stoichiometry in the $YBa_2Cu_3O_x$ compounds affects phonon spectra and as a result the value of dispersion of interlayer modes and the type of an absorption edge. Clearly, our model explaines the influence of stoichiometry on the character of the peaks discussed above. Unfortunately more or less detailed experimental investigation ( influence of the stoichiometry on an absorption process) in a low energy region with sufficient resolution has not been carried out yet.

In conclusion we would like to consider briefly the behavior of the function $\varepsilon_2(\omega)$ near the singularity. Let us expand the expression (66) in the vicinity of the pole in the powers $\omega - \omega^*$. After explicit calculations we obtain:

$$\epsilon_2 \sim (\omega - \omega^*)^{-1/2}. \tag{68}$$

This expression describes experiments better than the Drude model [46]. It is the presence of boson branches that is responsible for this exponent in the expression (68). This exponent is universal for every models containing local pairs.

# 7. Conclusion

Our investigations reveal two important points. First, it was shown that the supposition of the exsistence of the local pair band below narrow polaron one explains various experiments in YBaCuO. The value of the polaron bandwidth is about 19meV and local pair bandwidth is about 10meV.

Second, the mathematics of the local pair (bipolaron) theory was developed. The band structure of the bipolarons and the interaction vertex of the bipolarons with external fields are presented here. The momentum dependency of the vertex is essential at the experiment explanation.

# 8. Aknowlegments

The authors are grateful to Profs. A.S.Alexandrov, A.B.Krebs, P.E.Kornilovich and D.A.Samarchenko for the enlightening discussions.

This work has been supported in part by RFFI Grant No.97-02-16705.

# 9. Appendix

Let us consider conditions of the parameters in expression (67). As the value $\xi$ changes in the range from zero to unity considering the determination and the form of a boson spectrum (see Fig. 1 and (61)) this fact impose certain conditions on the parameters in the equation. There are two cases:

1. Only a larger root satisfies the condition $(0 \leq \xi_1 \leq 1)$. This is possible if

$$\begin{cases} \omega \geq E_i^{ph}(\pi) + E^b(\pi) \\ \omega \leq E_i^{ph}(0) \end{cases} \tag{69}$$

2. Both roots satisfy the condition $(0 \leq \xi_1, \xi_2 \leq 1)$. This is possible if

$$\begin{cases} \omega \geq E_i^{ph}(\pi) + E^b(\pi) \\ \omega \geq E_i^{ph}(0) \\ \omega \leq E_i^{ph}(0) + \frac{(E^b(\pi))^2}{4(E_i^{ph}(0) - E_i^{ph}(\pi))} \end{cases} \tag{70}$$

3. Only a smaller root satisfies the condition $(0 \leq \xi_1 \leq 1)$.

$$\begin{cases} \omega \leq E_i^{ph}(\pi) + E^b(\pi) \\ \omega \geq E_i^{ph}(0) \end{cases} \tag{71}$$

1. The first type process corresponds to the condition $\rho > 1$ (large phonon dispersion). In this case the dependence $E_{tot}(k)$ is of the type shown in Fig. 10. One can easily see that the process of absorption starts when $\omega = E_i^{ph}(\pi) + E^b(\pi)$, that is with transitions from the ground state to the edge of Brillouin zone (at $k = \pi$). In an energy range corresponding to system of inequalities (69), one should use $\xi_1$ root when substituting it in Eq. (66). Next energy subinterval is in the range from $E_i^{ph}(0)$ to the maximum value of $E_{tot}(k)$, that is corresponds to the second and the third inequality in system (70). In this case transitions from the ground state to those that are near the zone center are included in the absorption process and both roots $\xi_1$ and $\xi_2$ being used in Eq. (66). It has already been pointed out that stepwise threshold of absorption is the property of the first type process. One can easily see that transitions are prohibited when $\omega < E_i^{ph}(\pi) + E^b(\pi)$. When $\omega = E_i^{ph}(\pi) + E^b(\pi)$ according Eq. (66), $\epsilon_2$ becomes infinity.

2. The second type process is realized when $\rho < 1$ (small phonon dispersion). In this case the total energy at the edge of the zone turns out to be more than the energy $E_{tot}(0)$ and the beginning of the absorption process is connected with transitions to the states near the zone center. As in the case of the first type process the whole energy interval is subdivided into to subintervals. The first one is described by the system of inequalities (71) and the second one is described by the first and the third inequalities of the system (70). In accordance with these inequalities it is necessary to use roots $\xi_1$ and $\xi_2$ when substituting them into Eq.(66). Within the energy interval pointed out the value $\epsilon_2$ becomes infinity.

# References


[1] W.A.Little // Phys.Rev. A134, 1416 (1964). V.L.Ginzburg // Contemp.Phys. 9, 355 (1968).

[2] H.Frohlich // Phys.Lett. 26A, 169 (1968).

[3] J.R. Schrieffer et al. // Phys.Rev. **B39**, 11663 (1989).

[4] A.S.Alexandrov, A.B.Krebs // Uspehi.Fiz.Nauk **162**-5, 1 (1992),

[5] A.S. Alexandrov and Sir Nevill Mott // *High Temperature Superconductors and other Superfluids* (Taylor& Francis, 1994), A.S. Alexandrov, N.F. Mott // Supercond. Sci. Technol. **6**, 215 (1993).

[6] J.O.Sofo et al. // Phys.Rev. B45, 9860 (1992).

[7] M.Drechsler et al. // Ann.Phys. 1, 15 (1993).

[8] R. Micnas, J. Ranninger and S. Robaszkiewicz // Rev. Mod. Phys. **62**, 113 (1990),

[9] Jan de Boer, V.E.Korepin, A.Schadschneider // Phys. Rev. Lett. 74, 789 (1995).

[10] C.Verdozzi, M.Cini // Phys.Rev. **B51**, 7412 (1995).

[11] R.P.Fynman, *Statistical Mechanics*, California, Inst. of Techn. (1972).

[12] V.N. Popov, *Path integrals in quantum field theory and statistical physics*, Moscow (1976).

[13] C.A.R. Sá de Melo *et al.* // Phys. Rev. Lett. **71**, 3202 (1993),

[14] A.B.Krebs, S.G.Rubin // Phys.Rev. **B49**, 11808 (1994); P. Sethna // Phys.Rev. **B25**, 5050 (1982).

[15] R.L.Stratonovich // DAN USSR 115, 1097 (1957); J.Habbard // Phys.Rev. Lett. 3, 77 (1959).

[16] A.V. Svidzinski, *Space-inhomogeniens problems in a theory of superconductivity*, Nauka, Moskow (1982).

[17] R.V.Konoplich,S.G.Rubin // Univ. di Roma, IFNF, preprint No 1004 (1994),

[18] A.S.Alexandrov, S.G.Rubin // Phys.Rev. B47, 5141 (1993),

[19] A.A.Gorbatsevich, I.V.Tocatli // Sov. ZETP **103**, 702 (1993).

[20] A.S.Alexandrov, N.F.Mott // Int.J.Mod.Phys.**8**, 2075, (1994).

[21] A.V.Bazenov // Sov. ZETP, 102, 1040 (1992),

[22] J.Rossat-Mignot et al., Int. Workshop on the use of neutron and x-rey in the study of magnetism, Grenoble, 21-23 January, 1993.

[23] M.C.Gallagher, J.G. Adler, J. Jung, and J.P. Franck // Phys. Rev., **B37**, 7846 (1988).

[24] Tetsuya Hasegawa, Hideyuki Suzuki, Seiji Yaegashi at al.// Jpn. J. Appl. Phys, **28**, L179 (1989).

[25] T. Ekino,J. Akimitsu // Phys. Rev., **B40**, 6902 (1989).

[26] J.Geerk, X.X. Xi and G. Linker // Z. Phys.B, **73**, 329 (1988).

[27] J.R. Kirtley et al. // Japan. J. Appl. Phis., **26**, Suppl.26 (1987). J.R. Kirtley et al. // J. Vac. Sci. and Technol. Ser. A, **6**, 259 (1988).

[28] J. Takada et al. // Phys. Rev., **B40**, 4478 (1989).

[29] A.P. Fein J.R. Kirtley et al. // Phys. Rev., **B37**, 9738 (1988).

[30] M. Hurd, R.I. Shekhter and G.Wendin // Phys. Rev., **B46**, 8527 (1992).

[31] S.I.Mukhin, D.Reefman, L.J.Jongh // Physica C, **171**, 42 (1990).

[32] A.S.Alexandrov, M.P. Kazeko and S.G. Rubin // Sov. ZETF, **98**, 1656 (1990); A.S.Alexandrov, M.P.Kazeko, G.G., Melkonian // Sov. FTT, **34**, 3628 (1992).

[33] V.A. Khlus and A.V. Dyomin // Journal of Superconductivity, **8**, No. 1, 71 (1995).

[34] C. Zhou, H.J. Schulz // Phys. Rev., **B45**, 7397 (1992).

[35] A. Barone, G. Paterno, *Physics and Applications of the Josephson Effect* (New York: Wiley- Interscience 1982).

[36] A.A. Abrikosov, *Fundamentals of the Theory of Metals* (Nauka, Moscow, 1987).

[37] J.M. Valles, Jr. et al., // Phys. Rev., **B44**, 11986 (1991).

[38] D.Pines, *Elementary Excitations in Solids*, New York-Amsterdam (1963).

[39] E.Demler et al. // Phys.Rev.Lett. 75, 4126 (1995).

[40] A.S.Alexandrov, M.P.Kazeko, S.G.Rubin // Sov. ZETP **71**, 1656 (1990).

[41] to be published in Phys.Rev. B, April (1998).

[42] P.Bourges et al. // Phys.Rev. B53, 1 (1996).

[43] B.J.Sternlieb et al. // Phys.Rev. B50,12915 (1994).

[44] Hung Fai Fong et al. // Phys.Rev.Let.,75,316 (1995).

[45] M.Randeria et al. // Phys.Rev. B41, 327 (1990)

[46] E. Dagotto // Rev.Mod.Phys., Vol. 66, No. 3, p.799, (1994),

[47] A.V.Bazenov // Sov.SPCT, 6, 271, (1993).

[48] A. Animaly, *Intermediate quantum theory of crystalline solids*, Prentice Hall, Inc.,Englewood Cliffs, New Jersey (1977),

[49] Yu.A.Kataev, I.F.Limonov, A.P.Mirgorodski et al. // Sov. FTT, **35**, 865 (1994),

[50] A.V.Bazenov, L.V.Gasparov, V.D.Kulakovski et al. // Sov. Letters in ZETF, **47**, 162 (1988).

[51] L.P.Regnault et al. // Physica B 213/214, 48 (1995).

## FIGURE CAPTIONS

Fig.1. The band structure of 2 - particle coupled states in the 2 - dimensional case. Solid line - singlet bands, dashed lines - triplet bands. The interaction energies of fermions $U_{s1} = +8$; $U_{s2} = -6.8$; $U_{t2} = -6.5$; the fermion bandwidth $D_{pol} = 4$. The bottom of the 2-polaron continuum is placed at $E_{pol} = 4.05$. Unit: $1 = 5meV$. The momentum dependence of the excitation energy along the line:

a) $\mathbf{q} = (q_x, 0)$; b) $\mathbf{q} = (q, q)$.

Fig.2. The formfactors for the transitions from the lowest singlet band: 1) the local pair transition within the lowest singlet band, 2) the transition into the upper singlet band, 3) the allowed transition into the triplet band. The momentum dependence of the formfactor along the line $\mathbf{q} = (q_x, 0)$.

Fig.3. Tunneling from a superconductor ($S$) to normal metal ($N$). a) Bipolaron decay to a polaron in the polaronic band and an electron in the normal metal; b) Electron transition from a normal metal to bipolaronic superconductor.

Fig.4. $\frac{dJ}{dV}$ versus $V/T_c$ for different temperature $T$: $T/T_c = 0.05$ (1), $T/T_c = 0.17$ (2), $T/T_c = 0.55$ (3), $T/T_c = 0.75$ (4). $D/T_c = 1.87$, $\Delta/T_c = 1.04$, $W/T_c = 0.47$, $T_c = 85K$. a) $\gamma\rho = 2$; b) $\gamma\rho = 1.7$. Inset shows the dependence $\Delta_{eff}$ on $T/T_c$.

Fig.5. $\frac{dJ}{dV}$ versus $V/T_c$ for different $\gamma\rho$ calculated within the framework of the bipolaron model $\Delta/T_c = 1.06$, $D/T_c = 1.87$, $W/T_c = 0.4$, $T_c = 85K$. a) $\gamma\rho = 1.8$; b) $\gamma\rho = 1.28$. The dotted lines are the experimental curves [27].

Fig.6. $\frac{dJ}{dV}$ versus $V/T_c$ for different $T$ calculated on the basis of the bipolaron model. $\Delta/T_c = 3.2$, $D/T_c = 3.25$, $W/T_c = 2.8$, $T_c = 85K$, $\omega_0/T_c = 5$, $x = 0.5$.

Fig.7. The neutron intensity along the line $q_x = q_y$ at $\omega = 41meV$. Solid line - theory, points - experiment in $YBaCuO$ ($x = 0.97$) at $T = 4.2K$ [42].

Fig.8. The energy transfer dependence of the neutron intensity for momentum tranfer $\mathbf{q} = (\pi, \pi)$. $D/T_c = 1.9$, $Delta/T_c = 1$. Solid line - theory,

points - experiment in $YBaCuO$ ($x = 0.92$) at $T = 5K$ [51].

Fig.9. The temperature dependence of the neutron intensity at $q_x = q_y$, $\omega = 41meV$. Solid line - theory, points - experiment in $YBaCuO$ ($x = 0.97$) [42].

Fig.10. The total energy $E_{tot}(k) = E_i^{ph}(k) + E^b(k)$. Curve 1 - large phonon dispersion ($\rho > 1$), curve 2 - small phonon dispertion ($\rho < 1$).

Fig.11. The imaginary part of dielectric susceptibility $\varepsilon_2(\omega)$. An experimental dependence [21] (a). The theoretical dependence (b).

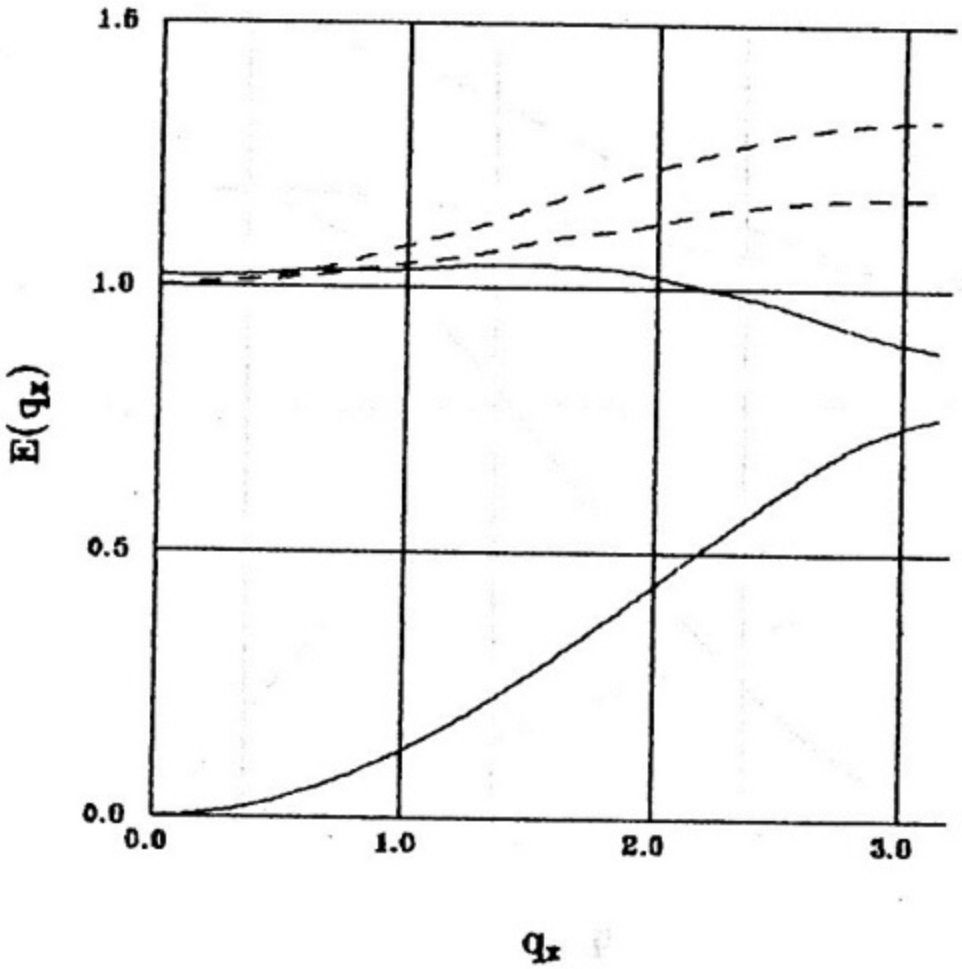


Fig.1a

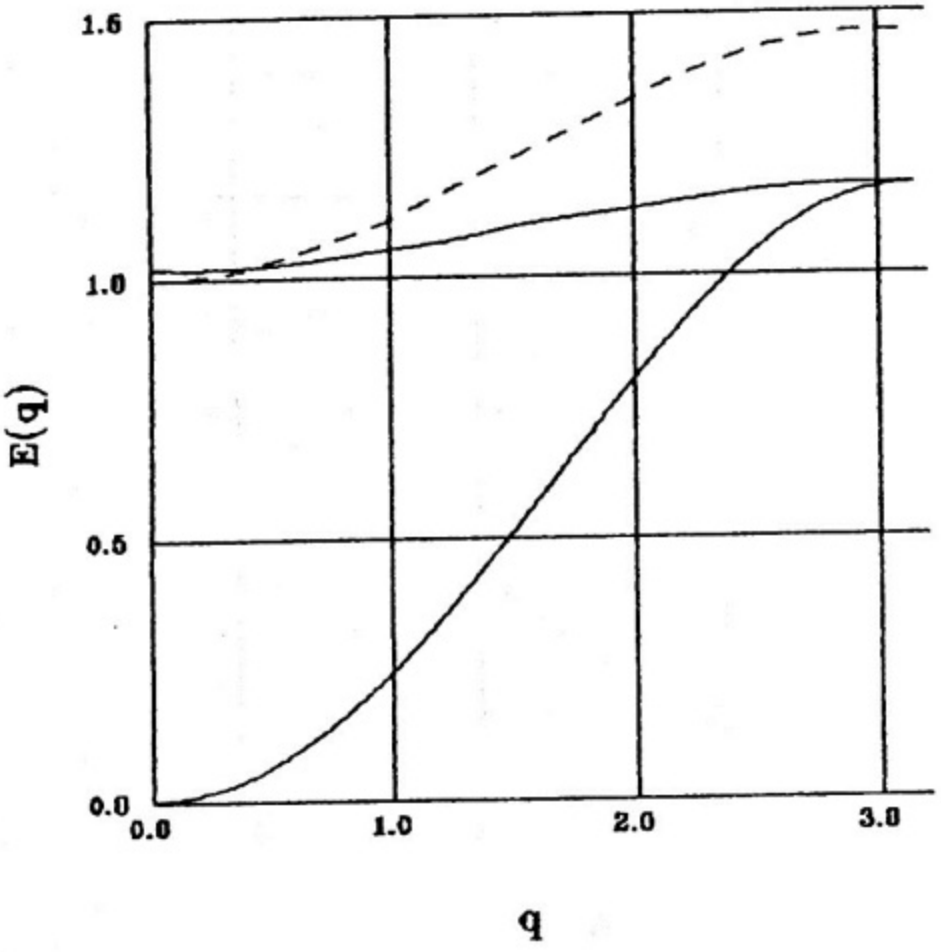


Fig.1b

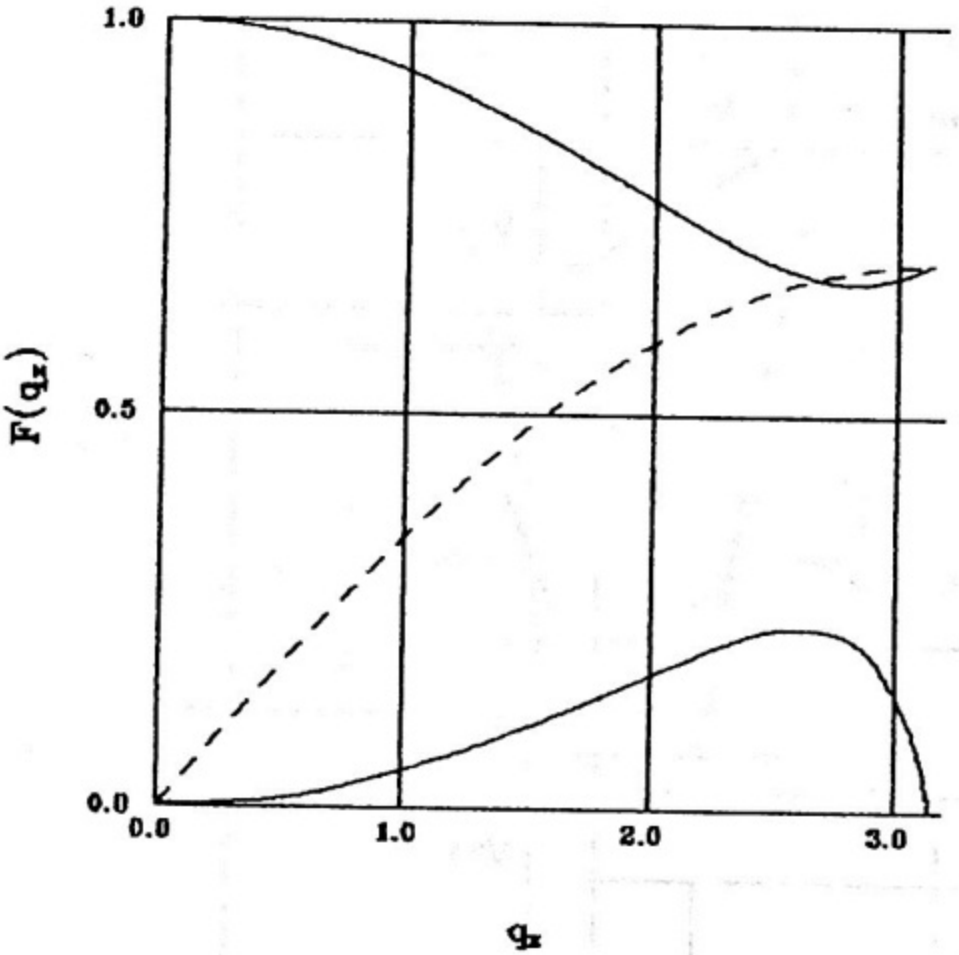


Fig.2

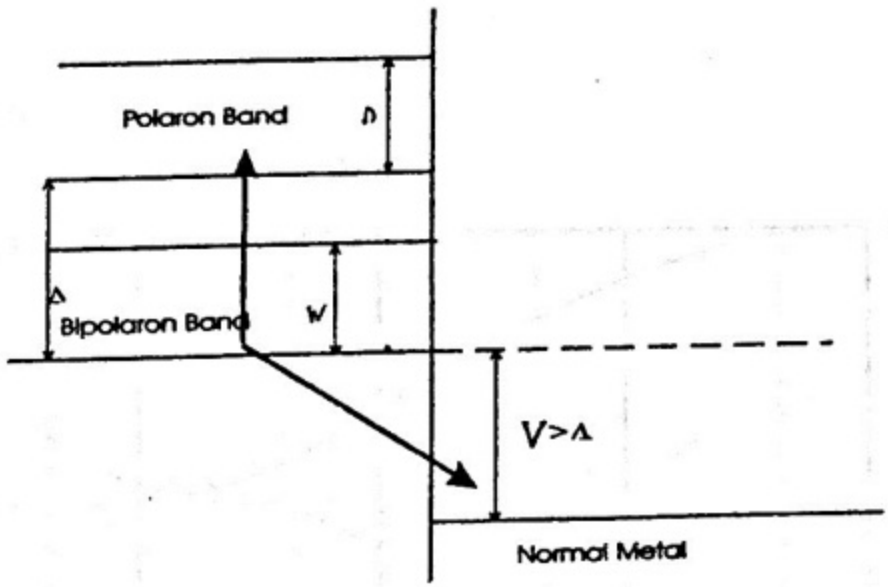


Fig.3a

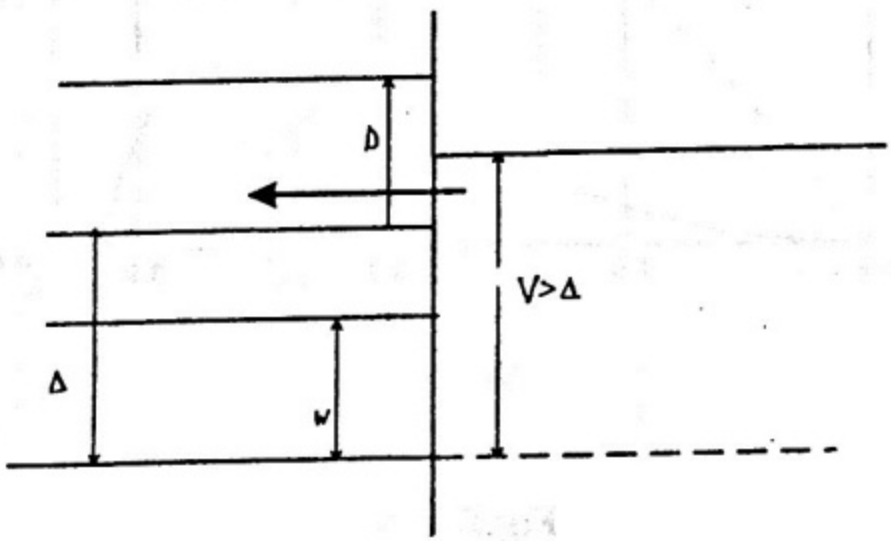


Fig.3b

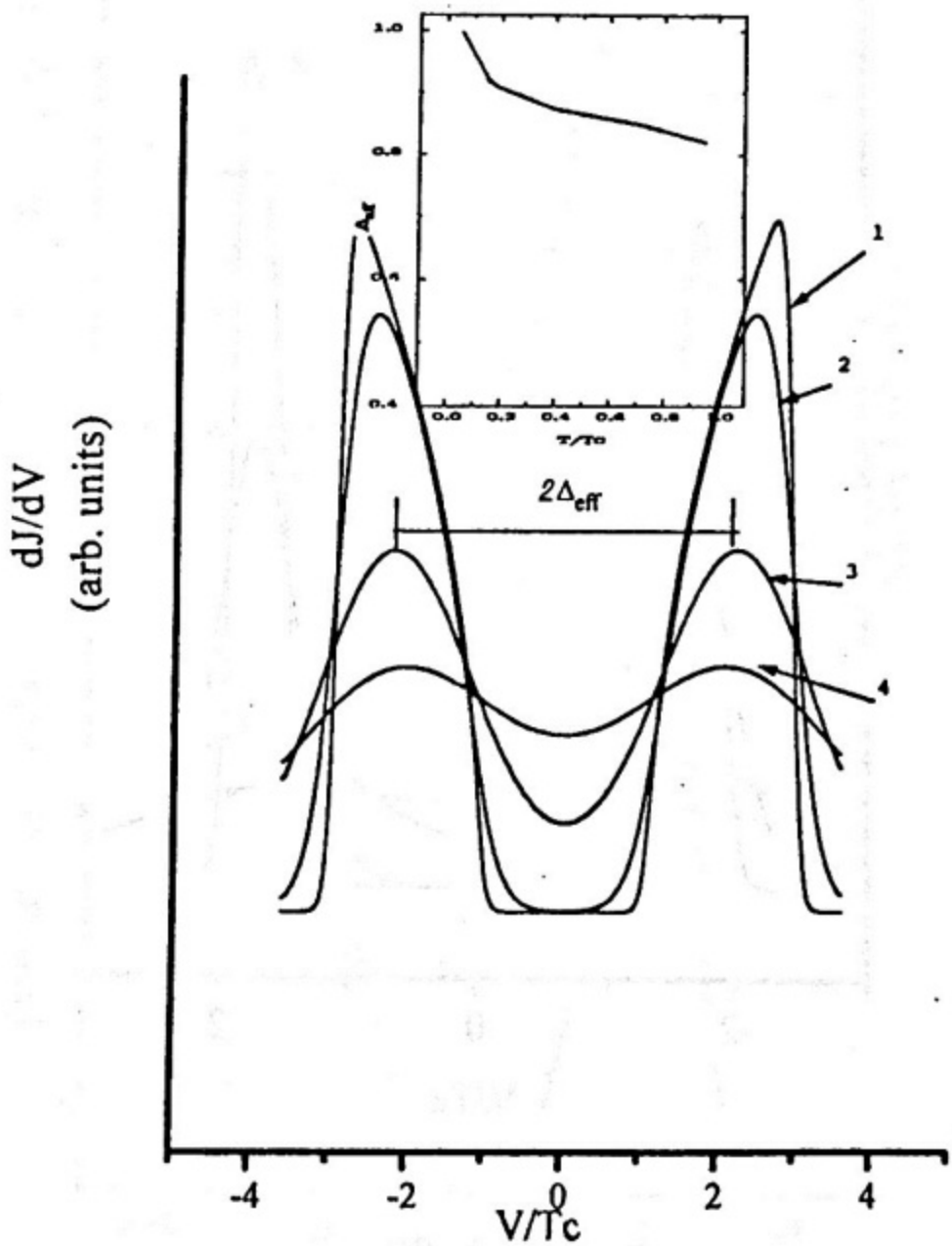
dJ/dV
(arb. units)
1.0
0.8
0.6
0.4
Δ/Δ0
0.0
0.2
0.4
0.6
0.8
1.0
T/Tc
2Δeff
1
2
3
4
-4
-2
0
2
4
V/Tc

Fig.4a

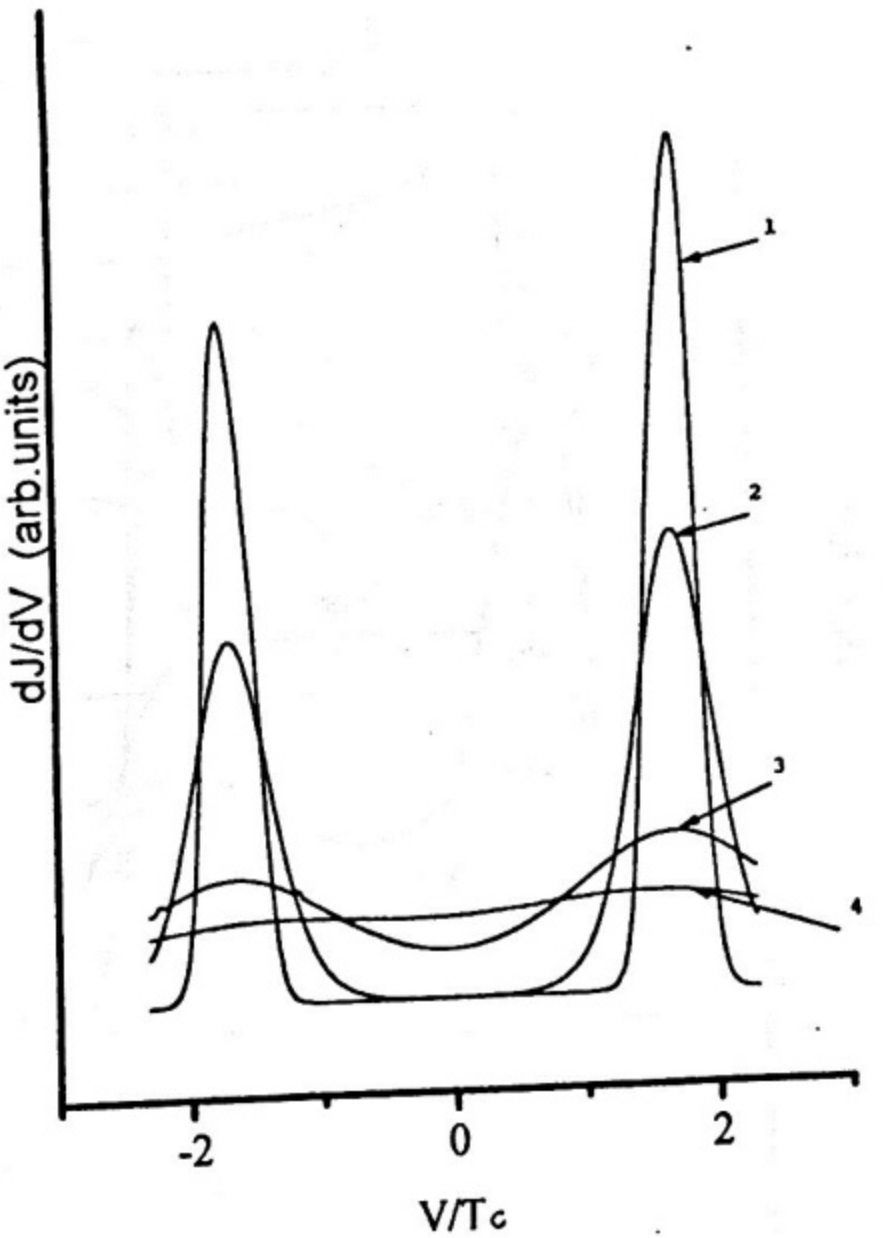


Fig.4b

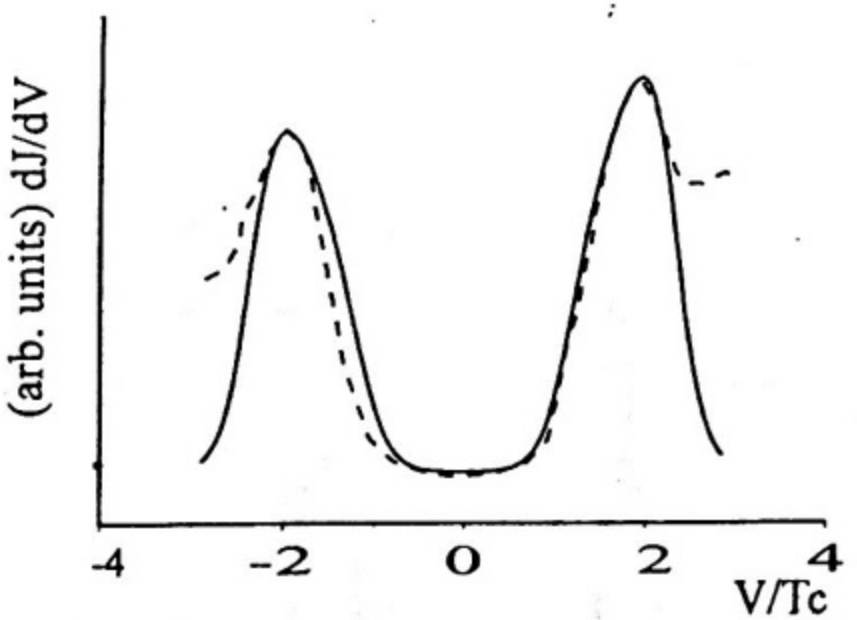


Fig.5a

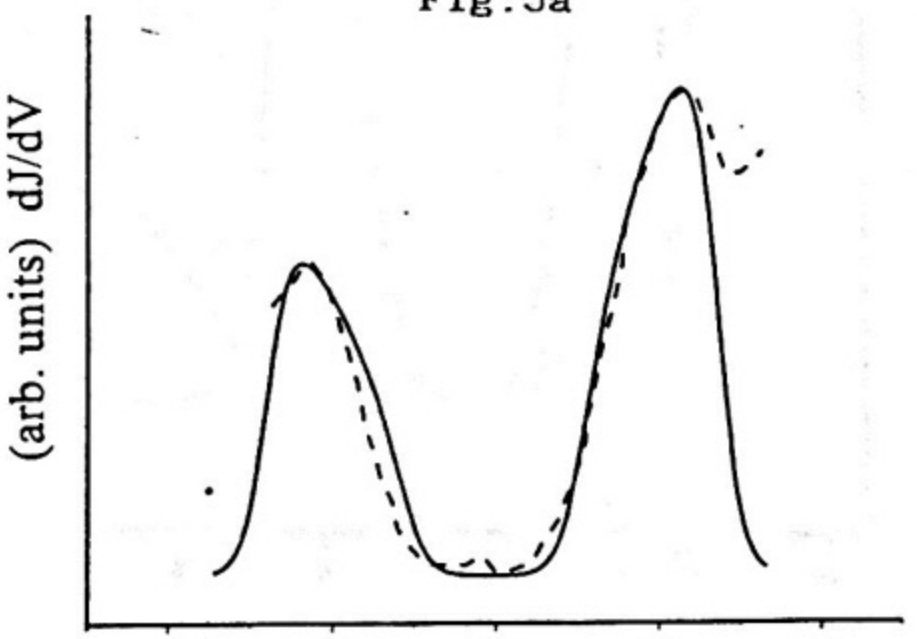


Fig.5b

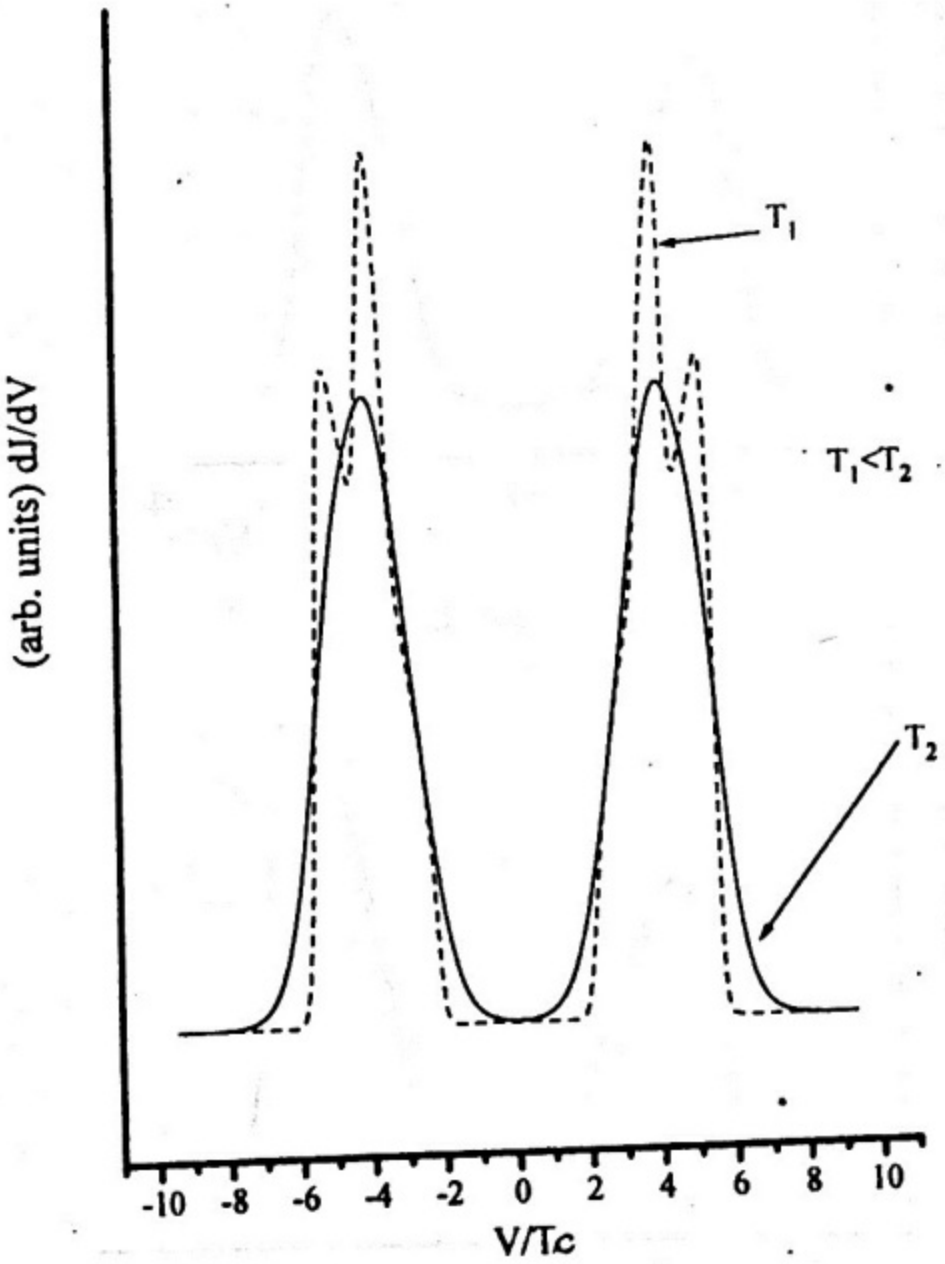


Fig.6

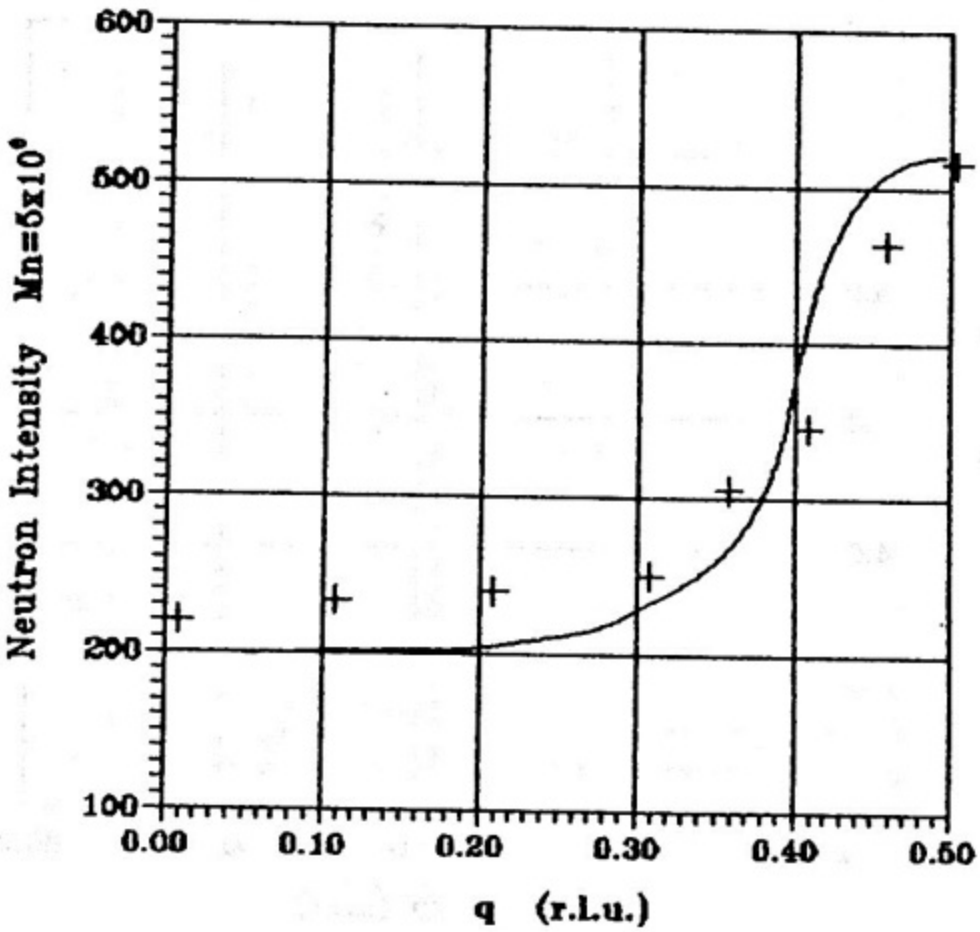
Neutron Intensity Mn=5x10⁶
600
500
400
300
200
100
0.00
0.10
0.20
0.30
0.40
0.50
q (r.l.u.)

Fig.7.

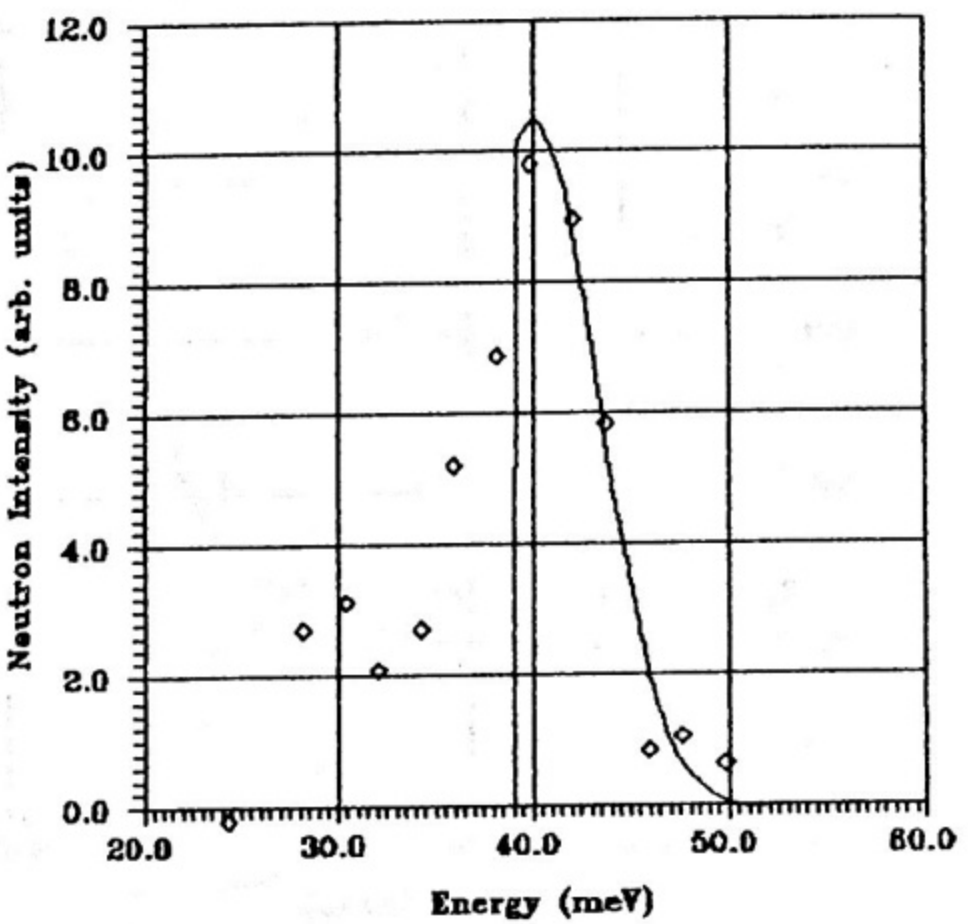
12.0
10.0
8.0
6.0
4.0
2.0
0.0
Neutron Intensity (arb. units)
20.0
30.0
40.0
50.0
60.0
Energy (meV)

Fig.8.

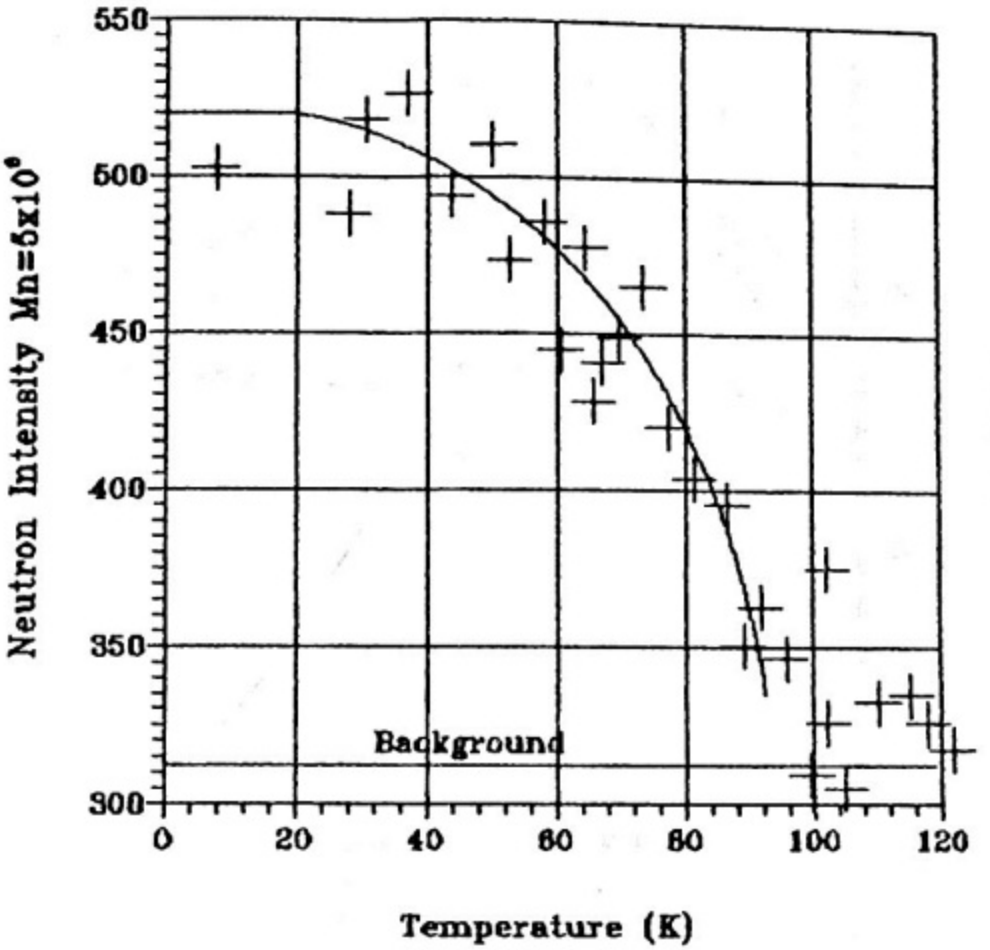
Neutron Intensity Mn=6x10⁶
550
500
450
400
350
300
0
20
40
60
80
100
120
Background
Temperature (K)

Fig.9

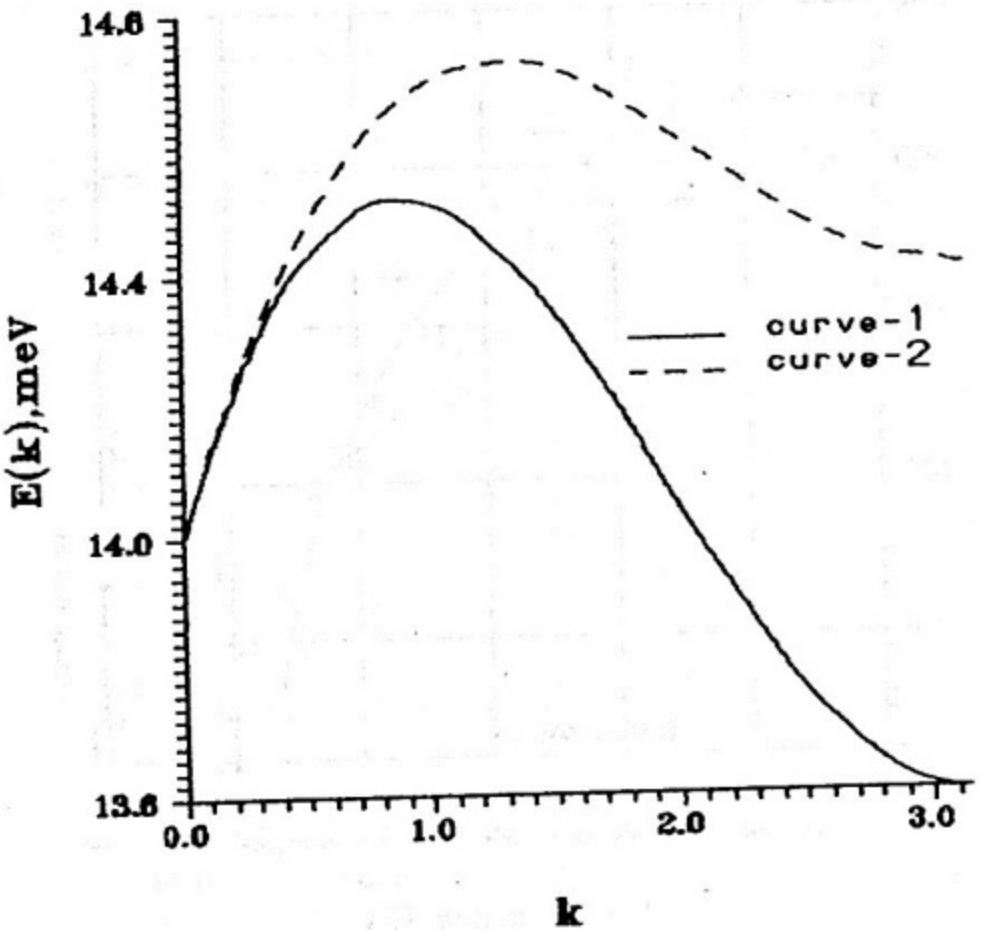


Fig.10

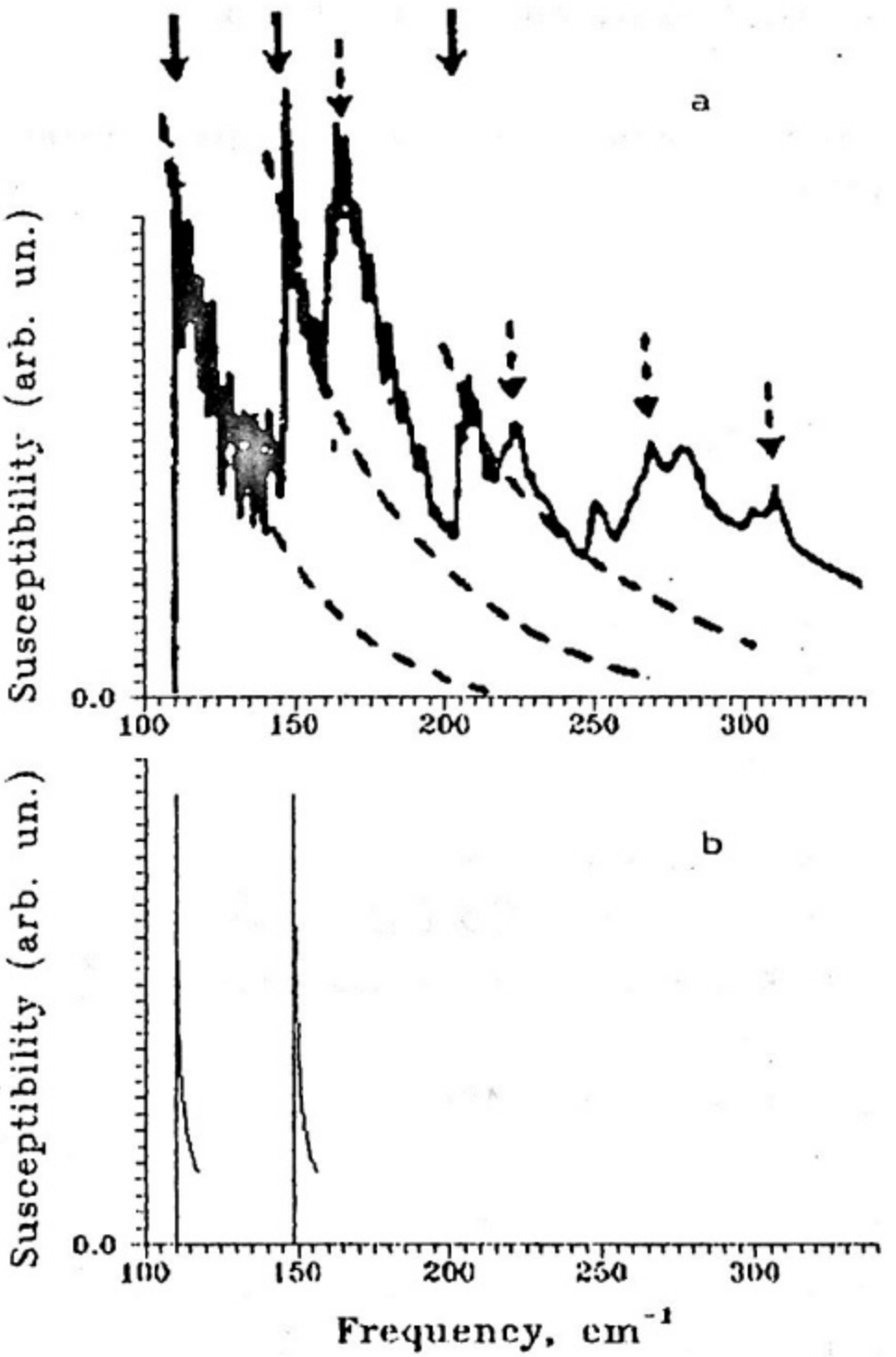
a
b
Susceptibility (arb. un.)
Susceptibility (arb. un.)
0.0
0.0
100
150
200
250
300
100
150
200
250
300
Frequency, cm$^{-1}$

Fig.11

Sergei.G. Rubin, Andrei.G. Terekidi.

Bipolaron theory and its application in $YBA_2CU_3O_{6+x}$.

Рукопись поступила в издательский отдел
01.12.97.

Редактор Н.Н. Антонова
Ответственный за выпуск А.Г. Терекиди

ЛР № 020678 от 09.12.92.
Подписано в печать 03.02.1998
Формат 60X84 1/16 Уч.-изд.л.3,5 Печ.л.3,75
Тираж 100 экз.
Изд. № 024-97 Заказ 101

Московский государственный инженерно-физический институт (технический университет). Типография МИФИ.

115409. Москва. Каширское ш., 31